Joint Centre for Mesoscale Meteorology, Reading, UK

Use of water vapour imagery and PV inversion to adjust initial conditions in NWP

S. J. Swarbrick

Internal Report No. 102

February 1999

Met Office Joint Centre for Mesoscale Meteorology Department of Meteorology
University of Reading PO Box 243 Reading RG6 6BB United Kingdom
Tel: +44 (0)118 931 8425 Fax: +44 (0)118 931 8791
www.metoffice.com

Designed and produced by the Met Office © Crown copyright 2001 01/0240 The Met Office logo is a registered trademark.

Use of Water Vapour Imagery and PV Inversion to Adjust Initial Conditions in NWP

Interim Project Report

Sean J Swarbrick

UK Met Office / Joint Centre for Mesoscale Meteorology

Feb 1999

Abstract

It is considered generally desirable to make greater use of satellite imagery in the generation of NWP analyses. This project is exploring one possible way of doing this, using the Meteosat water vapour channel. The technique attempts to utilise the alleged relation between WV imagery and upper-tropospheric PV fields. This relation, if properly understood, should facilitate the detection of errors in the initial state of a forecast.

The PV field on an appropriate isentropic or isobaric surface, at the initial forecast time, is compared with the corresponding WV image in order to reveal errors in the PV field. The PV field is then adjusted accordingly, and PV inversion is used to derive wind and temperature adjustments from the PV adjustments. The PV adjustments may involve scaling and/or displacement of PV anomalies, on a range of pressure levels. The resulting wind and temperature adjustments are applied to the initial forecast fields, and the forecast is rerun from the adjusted initial state.

A number of case studies have been carried out, and some positive impacts have been achieved, although the results as a whole seem to suggest that upper-tropospheric PV adjustment by itself may not lead to a positive impact in general.

It has also become apparent that the relation between PV fields and water vapour images is not well understood, and that a correct understanding of this is essential to further progress. Some significant qualitative insights on this issue have emerged.

Author's address: JCMM, Dept. of Meteorology, University of Reading, PO Box 243,
Reading RG6 6BB, UK Tel. 01189 316524
email: sjswarbrick@meto.gov.uk

CONTENTS

1. INTRODUCTION
Scientific Basis of the Project;
The PV - WV Image Correlation 1

2. OVERVIEW OF TECHNIQUES 5

2.1 Introduction 5
2.2 The WV Image / PV Comparison 6
2.3 PV Modification 6
2.4 PV Inversion and Initial Field Adjustment 7

3. THE PV - WV IMAGE RELATION AND APPROACHES TO PV ADJUSTMENT 9

3.1 The Relation Between Water Vapour Images and Upper-Tropospheric PV 9
3.2 Approaches to PV Adjustment 12
3.3 Possibilities for Automated PV Adjustment 15

4. THE PV INVERSION TECHNIQUE 17

4.1 The PV Inversion Program 17
4.2 Difficulties with the PV Inversion Technique 19

5. OVERVIEW OF CASE STUDIES 23

5.1 Concise Summary of Cases 24
5.2 Detailed Accounts of Case Studies 26

6. CONCLUDING SUMMARY 45

References 49

List of Figures

Chapter 3 (after p. 16)

Fig. 3.1 PMSL analysis, 6z 20/10/97
Fig. 3.2 Conceptual model of PV anomaly and dry intrusion
Fig. 3.3 Background WV image 6z 20/10/97; Contours PV on 250hPa
Range 0-12 PVU, Interval 1 PVU
Fig. 3.4 Background WV image 6z 20/10/97, Contours PV on 400hPa
Range 0-5 PVU, Interval 1 PVU

Chapter 5

Case 4 (after p. 30)

Fig. 5.4.1 Case 4 PMSL analysis 12z 1/9/97
Fig. 5.4.2 Case 4 PMSL analyses, 12hr intervals from 0z 2/9/97
Fig. 5.4.3 Case 4 PMSL original forecast T+12 to T+48
Fig. 5.4.4 Case 4 Background WV image 12z 1/9/97
Contours PV at 300hPa, from analysis
Range 0-12 PVU, Interval 1 PVU
Fig. 5.4.5 Case 4 Rerun 3 Background WV image 12z 1/9/97
Contours PV on 300hPa
Range 0-12 PVU, interval 1 PVU
Fig. 5.4.6 Case 4 Rerun 3 PMSL T+12 to T+48

Case 6 (after p.33)

Fig. 5.6.1 Case 6 PMSL analysis 12z 15/9/97
Fig. 5.6.2 Case 6 PMSL analyses, 12hr intervals from 0z 15/9/97
Fig. 5.6.3 Case 6 PMSL original forecast T+12 to T+48
Fig. 5.6.4 Case 6 Background WV image 12z 15/9/97
Contours PV at 300hPa, from analysis
Range 0-12 PVU, Interval 1 PVU
Fig. 5.6.5 Case 6 PV on 250 & 300hPa 12z 15/9/97
Range 0-12 PVU
Fig. 5.6.6 Case 6 Rerun 1 PV on 250 & 300hPa T+0
Range -4 -12 PVU
Fig. 5.6.7 Case 6 Rerun 1 PMSL T+12 to T+48

Case 11 (after p. 40)

Fig. 5.11.1 Case 11 PMSL analysis 6z 13/10/97
Fig. 5.11.2 Case 11 PV on 250hPa T+0
Upper: Original field Lower: Rerun 1
Fig. 5.11.3 Case 11 PMSL analyses, 6hr intervals from 12z 13/10/97
Fig. 5.11.4 Case 11 PMSL original forecast T+6 to T+24
Fig. 5.11.5 Case 11 Background WV image 6z 13/10/97
Contours PV at 300hPa, from analysis
Range 0-12 PVU, Interval 1 PVU
Fig. 5.11.6 Case 11 Rerun 1 PMSL T+6 to T+24
Fig. 5.11.7 Case 11 Cyclone at 6z 14/10/97
Analysis, original forecast, rerun 1

1. INTRODUCTION

The process of generating an NWP analysis by data assimilation is sometimes adversely affected by lack of observations at important locations, such as those at which significant cyclonic development is occurring. Oceanic regions in particular may suffer from lack of adequate observations; this is particularly pertinent for UK weather, for which one of the major controlling influences is the North Atlantic 'storm track', along which cyclones develop and travel eastwards. It would therefore seem desirable to make greater use of satellite imagery as a data source for NWP. Satellites provide blanket coverage over vast areas of the earth; Meteosat, for example, is a geostationary satellite whose images cover most of the N Atlantic area.

Hitherto, satellite images have been used by the human forecaster as a valuable aid in assessing the state of the atmosphere. If satellite data could also be exploited in the context of NWP, this could significantly enhance the accuracy of computational forecasting. The question is, how could this be achieved in practice? Satellite image data is usually in the form of radiance or brightness temperature fields, which have to be interpreted in some way to render them meaningful for a forecasting model, which is formulated in terms of meteorological variables such as pressure, temperature, wind velocity and humidity.

In principle, there are various possible ways of incorporating satellite image data into a NWP model. The purpose of this project is to explore the feasibility of one of these possibilities. The method envisaged makes use of one particular type of satellite imagery, namely the Meteosat water vapour channel. The objective of this method is to obtain wind and temperature increments which can be used to adjust the NWP model's initial state in a balanced and consistent manner, and which will make that initial state conform more closely to the actual state of the atmosphere, as revealed by the imagery. In particular it is hoped that such adjustments would lead to more accurate representations of so-called "tropopause folds", which are important in connection with cyclonic development.

Scientific Basis of the Project; the PV - WV Image Correlation

The process of obtaining wind and temperature increments from WV images has two main stages. The first stage exploits the supposed relationship between water vapour imagery and upper-tropospheric potential vorticity fields. This relationship, if properly understood, should enable errors in the NWP model's analysed upper-tropospheric PV fields to be detected, since such errors would appear as 'mismatches' between the PV distribution and the WV image. PV adjustments could then be made to correct these errors. The second stage involves PV inversion, by means of which the PV adjustments are converted to wind and temperature increments. These increments are then used to adjust the model's initial state.

The relationship between PV fields and WV images has been widely explored by many authors; in particular, Demirtas (1996), Demirtas and Thorpe (1997), Georgiev (1996), Rosting et al. (1996), Schmetz and van de Berg (1994). A WV radiance field is produced by radiation integrated over the depth of the upper troposphere, generally from about 250hPa - 500hPa. The stratosphere has very little water vapour and so produces no significant emission at this wavelength. Radiation from below the 500hPa level is reabsorbed as it propagates upwards. A WV image therefore represents the humidity distribution of the upper troposphere. In general, low

humidity regions have the highest brightness temperatures, since the observed radiation in such regions has originated from lower (and therefore warmer) levels. Intrusions of dry stratospheric air into the troposphere, which occur in association with tropopause folds, therefore appear as high brightness temperature features on WV images. Since stratospheric air has high PV (due to high static stability), there should be a correlation between high PV at upper-tropospheric levels and high BT regions in the WV image.

Consideration must be given to the question of which upper-tropospheric surface is the most appropriate one to use for the PV - WV image comparison. Intrusions of stratospheric air into the troposphere occur in the vicinity of the jet stream, so the PV - WV relation is valid only in this vicinity. Climatology indicates that isentropic surfaces in the 315K/330K range intersect the tropopause at jet stream latitudes. Isentropic surfaces in this range are therefore suitable for the comparison of PV fields with WV imagery. In winter the 330K surface is likely to be better, in summer 315K is preferable (Demirtas 1996). In practice, PV adjustment is carried out on isobaric, rather than isentropic surfaces, since the PV inversion algorithm which this project uses is formulated on pressure levels (Ziemanski 1994). PV fields on the 300/250hPa surfaces are generally similar to those on 330/315K, so they can also be used for the PV -WV image comparison.

The PV - WV relation is not very well defined in general, and is, as yet, purely qualitative, although quantitative investigations are being carried out by other projects related to this one. It is also, of course, merely a two-dimensional relation, which is a significant limitation, as any PV adjustments must be carried out over a range of vertical levels. Chapter 3 of this report discusses the PV - WV relation in more detail, including the issues touched on here.

The PV inversion procedure also has various caveats and uncertainties associated with it, which are discussed in chapter 4.

Background to the Project

This project was suggested by the PhD work of Meral Demirtas, a research student of Prof. A. Thorpe of Reading University Dept. of Meteorology (Demirtas 1996, Demirtas and Thorpe 1997). Demirtas carried out a small number of case studies involving PV adjustment in relation to WV imagery, and the use of PV inversion to derive wind and temperature fields from the adjusted PV fields. Some significant positive impacts on forecasts of cyclonic development were obtained.

Demirtas' work provided a starting point for this project, although there have been a number of major technical improvements in the methodology. Demirtas carried out PV adjustment and PV inversion on the JCMM 'DISP' graphics system grid, and input the resulting winds and temperatures to the Unified Model as "dummy observations" via the AC assimilation scheme. This procedure was unsatisfactory in a number of ways. The DISP grid has, in general, a much coarser resolution than the UM grid, which severely limited the level of detail possible in the PV adjustments. The total number of dummy observations which the AC scheme would accept was also limited. Furthermore, the AC scheme does not allow dummy observations to pass through into the UM analysis unaltered; the nudging and balancing algorithm which the AC scheme employs attenuated the wind and temperature adjustments generated by PV inversion to a considerable extent.

Initially, this project also employed the DISP system, since this was the only graphics facility available which allowed satellite images to be overlaid by UM field contours, and so was the only means by which the PV - WV image comparison could be made. However, this capability was subsequently incorporated into the JCMM 'PPLOT' graphics facility, which uses pp files generated by the UM, and so enables the PV - WV comparison to be carried out on the UM grid. This also enables PV adjustment to be carried out directly on the UM grid, and so wind and temperature adjustments can be derived at UM gridpoints. These adjustments can then be applied directly to the analysis fields in a UM dump file, so eliminating the need to rely on the AC assimilation procedure. The use of PPLOT rather than DISP thus overcame these technical disadvantages which Demirtas' work was subject to.

The derivation of wind and temperature adjustments on the UM grid rather than the DISP grid also required developments to the PV inversion algorithm, which were carried out by M Griffiths (Griffiths et al. 1998); an account of these is given in chapter 4.

2. OVERVIEW OF THE TECHNIQUES USED IN THE PROJECT

2.1 Introduction

In order to assess the effectiveness of the PV/WV methodology, a sequence of case studies has been undertaken. Most of the cases discussed in this report are vn4.3 LAM forecasts from September/October 1997. In the earlier cases a 48 hour forecast period was studied, while in the later cases this was reduced to 24 hours. In general these cases were selected at seven day intervals. The objective of this systematic selection of cases was to provide an unbiased range of meteorological situations, rather than to deliberately seek out cases which looked 'promising' from a PV perspective.

The reason for using the LAM rather than the global UM was simply because this project was initially approached as a follow-on from M. Demirtas' work, which used the LAM (Demirtas 1996, Demirtas and Thorpe 1997). Having decided to use the LAM, it followed that selection of cases was restricted to the period from summer 97 to Feb. 98, since this was the duration of the LAM's operational existence on the T3E. It was in fact decided to begin the sequence from Sept 1st. 97. It is intended that future case studies will utilise the vn4.4/4.5 global UM, which will require some alteration to the software utilities which the project employs.

The sequence of steps involved in a case study is as follows:

(a) Compare the forecast with corresponding analyses, at 6 or 12 hour intervals, in order to decide which forecast errors to focus on. (This step is optional, but thus far has always been carried out).

(b) Compare the analysed upper tropospheric PV fields at T+0 (and possibly at other times as well) with the corresponding satellite water vapour image. Decide what adjustments to make to the PV fields.

(c) Generate the adjusted PV fields (a partly manual process).

(d) Invert the original and the adjusted PV fields (corresponding to T+0). Each inversion outputs a set of wind and temperature fields on a range of pressure levels, which are then interpolated to model levels.

(e) Compute the differences of the two sets of wind and temperature fields on model levels, to provide fields of increments.

(f) Add the increment fields to the initial analysis, to provide an adjusted initial analysis for a rerun.

(g) Rerun the forecast from the adjusted initial analysis.

(h) Compare the output fields from the rerun with the original forecast and analyses.

The technical procedures involved in some of the above steps will now be described in more detail.

2.2 The WV Image / PV Comparison

The satellite water vapour image for the appropriate time is plotted using a colour scheme to represent brightness temperature. The colour scheme shows higher brightness temperatures as yellow, orange and red, and lower ones as green and blue. Higher brightness temperature usually corresponds to drier air, at N Atlantic storm track latitudes. Dry intrusions of stratospheric origin will thus appear in the yellow-red range, provided the air above them is clear of cloud. Anticyclonic regions will also appear in yellow-red colours, since the air in such regions is warmed by adiabatic descent.

The image is affected by the presence of cloud, which appears as green or blue on the image. Dry air is often obscured by overlying cloud. It should be noted that moist regions and cloudy regions are of interest as well as dry regions (because they help to diagnose stages of cyclonic development, etc.).

The WV image is overlaid with contours of the PV field for an appropriate isentropic surface (usually 330K) or a related pressure surface (250 or 300 hPa). In general, a case study focuses on a particular feature of the cyclonic development. It is usually possible to relate this to a particular PV anomaly visible at upper-tropospheric levels. Any particular PV anomaly is usually associated with a dry feature in the water vapour image. By examining the disposition of the PV contours relative to the WV image, and the structure of the PV field on a range of levels from 250 to 500 hPa, it is generally possible to interpret the relation between the WV image and the PV field. This is discussed in more detail in chapter 3.

2.3 PV Modification

Examination of the PV fields and other fields at the initial forecast time, and also as a time sequence, as well as of the PV/WV image comparison, enables a judgement to be made as to how the initial PV fields may be modified in order to influence the forecast in a particular way. The actual modification is carried out by reading the PV field data from a pp file, altering selected field values by scaling, translation, or overwriting, and then writing out the adjusted field to another pp file. The process of selecting which field values are to be altered, and deciding how to alter them, involves manual judgement and so is inevitably crude and of limited scope. For example, it is relatively easy to scale or translate a well-defined PV anomaly by this method, but it is extremely difficult to alter the shape of PV contours (this has not been attempted in any of the case studies).

The PV inversion algorithm is formulated on (exner) pressure levels, so PV field adjustment must be carried out on a range of pressure levels. The PV/WV image relation is alleged to be valid for PV on isentropic surfaces in the approximate range 315K/330K. In practice, it is generally also valid for upper tropospheric isobaric surfaces, particularly around 300hPa, since such surfaces often intersect the tropopause (defined as the PV=2 surface) in the jet stream vicinity.

Having decided on an adjustment to the PV field on one such surface, usually 250 or 300hPa, it is then necessary to decide on corresponding adjustments to be made on lower surfaces, usually down to 500hPa. The PV/WV image comparison only provides guidance relating to a single 2-d surface, it does not yield any information about how the PV adjustments should vary in the vertical. This is another source of

uncertainty in PV adjustment, in addition to the uncertainties associated with the PV adjustments on the 2-d surface itself.

In practice, this problem is addressed in the following way. Having identified the PV element which is to be adjusted on the first pressure level (usually 250 or 300hPa), the vertical structure of this element is determined by examining its disposition on lower levels. In particular the slope and depth of the PV element are required. Any PV displacements made on the first pressure surface would also be made on the lower surfaces, if necessary allowing for the slope of the PV element. (In the case studies, it was found that most PV anomalies have an almost vertical structure). If a scaling factor is applied on the first surface, then a scaling factor would also be applied on the lower surfaces; the scaling factor may vary from level to level. Sometimes it may be considered desirable to extend the vertical depth of a PV element (this was done in case studies 4 & 7, see chapter 5).

2.4 PV Inversion and Initial Field Adjustment

The next stage is PV inversion, which enables a set of wind and temperature fields to be derived from a 3-d PV distribution subject to specified boundary conditions. The input data for the PV inverter is a set of PV fields on 19 pressure levels from 100hPa to 1000hPa. The output is a set of wind and temperature fields on the same pressure levels, which are then interpolated onto model levels.

PV inversion is carried out on both the original set of PV fields and on the adjusted set of fields. The differences of the two sets of output fields are then obtained, to give fields of increments which may be added to the initial fields for the forecast. The main reason for using the 'increment' approach to initial field adjustment is that the PV inverter computes only the non-divergent part of the wind, and the divergent part would therefore be lost if the initial wind fields were simply overwritten with values derived from inversion of the adjusted PV.

The fields of wind and temperature increments so obtained are added to the initial wind and temperature fields for the UM forecast, and the forecast is rerun from this adjusted initial state.

3. THE PV - WV IMAGE RELATION AND APPROACHES TO PV ADJUSTMENT

3.1 The Relation Between WV Images and Upper-Tropospheric PV

Experience gained thus far in this project indicates that the relation between upper-tropospheric PV fields and WV images is very complex and far from being well understood. As yet no positive impact has been achieved in any case study by displacing a PV element from its analysed position to another position. Positive impacts have been achieved in a few cases, but only by scaling PV elements without significantly altering their positions. The PV - WV image relation, in as far as it is understood at all, remains essentially qualitative. To be of any practical use, it would have to be quantified in some way, and the PV adjustment process automated. Attempts to quantify and automate PV adjustment are being pursued by related projects, brief details of which are given later in this chapter.

Various authors have written accounts of the PV - WV relation which can seem vague or even misleading. Examples can be found in Appenzeller and Davies (1992), Demirtas (1996), Demirtas and Thorpe (1997), Davis and Emanuel (1991), Morgan and Nielsen-Gammon (1998), Rosting et al. (1996), among others. Some of these authors make statements which appear to suggest that they believe in a simple superposition relation between upper-tropospheric PV elements and WV image elements. The statistical studies reported by Georgiev (1996) suggest that a one-to-one relationship between WV imagery and PV fields is not valid; for example, there is a dependency upon latitude and the vertical height of the PV field.

The qualitative perspective on the PV - WV image relation which has emerged from this project is best illustrated by considering a specific case. A suitable case for this purpose is the LAM analysis of 6z 20/10/97. In this case the 24 hour pmsl forecast had very little error and so the relation between the upper-tropospheric PV and the WV image can probably be regarded as a "good fit". No reruns have yet been attempted for this case but it is of interest to study the PV-WV relation to see how it illustrates the conceptual view of this which has emerged so far. The WV image and PV fields both show a number of structures which are typical of various of PV - WV image relationships.

It is also of interest to examine this case in relation to the 'rules' governing the PV - WV image relation used by M. Demirtas (Demirtas 1996, Demirtas and Thorpe 1997). These rules seem to provide a starting point for understanding the PV-WV relation, but they require some expansion and interpretation. The 'Demirtas rules' are as follows; they have been taken from the references stated here, but partially reworded. Note that 'BT' refers to brightness temperature.

Rule (1): Dry stratospheric air of high PV is seen as a high BT region on the WV image. There is also a close relationship between dry regions on the WV image and high PV values at the rear of a developing cyclone.
Note: The expression "close relationship" is an exact quote from Demirtas and Thorpe (1997). At first sight it is not clear what, precisely, is meant by this term. The nature of this close relationship is explored in the discussion which follows below.

Rule (2): The main PV gradient often coincides with the cloud edge/moist boundary. Frontal cloud is associated with low PV air, partly because it forms within an air mass of subtropical origin, and partly because latent heat release concentrates low PV

aloft. The latent heat mechanism is particularly relevant for sharp PV gradients associated with comma clouds in developing cyclones.

Rule (3): The PV gradient on an appropriate isentropic (or isobaric) surface tends to be concentrated on the warm side of high BT strips associated with the bases of upper troughs.

3.1.1 WV Image and PV Fields for the 6z 20/10/97 LAM Case

There are four dry intrusion-type features on the WV image, each with an (apparently) associated upper-tropospheric PV structure. It is useful to compare the PV-WV relation on 250hPa (fig. 3.2) with that on 400hPa (fig. 3.3), since the 250hPa level intersects large regions of the stratosphere, whereas the 400hPa level is mainly in the troposphere. There are some uncertainties in the interpretation which follows, but nonetheless a number of useful observations can be made.

The pmsl plot for 6z 20/10/97 (fig. 3.1) shows a large complex low pressure system stretching across the Atlantic from Biscay to Newfoundland, and extending as far south as the latitude of Gibralter. At least three of the dry intrusion features are clearly associated with this system, and so undoubtedly represent cyclonic development. The fourth dry feature appears to be associated with another cyclonic system just visible in the extreme NE of the pmsl plot.

Dry feature no.1

The large curving dry feature in the centre of the WV image partly overlaps a very intense PV anomaly on the 250hPa level. A possible interpretation is that the intense PV anomaly represents a dip in the tropopause, while the dry feature represents an intrusion of stratospheric air which is flowing around the tropopause dip (presumably having emerged from the tropopause dip at some level). The 250hPa level intersects the upper part of the tropopause dip, and so passes above a considerable depth of stratospheric air within the dip; hence the very high PV maximum. This PV maximum appears as a 'pivot point' for the circulation of the stratospheric intrusion. On the 250hPa PV field, a smaller PV maximum of 2-3 units can be seen to the west of the main anomaly, lying within the dry feature. This may be the PV signature of the dry intrusion itself, but the PV signature of the tropopause dip is by far the dominant feature at this level. On the 400hPa PV field the pattern has shifted somewhat; the PV maximum associated with the tropopause dip can still be seen at the eastern end of the dry intrusion, but it is now more comparable in prominence with the adjacent PV maximum associated with the dry intrusion air itself. The 400hPa level intersects the lower part of the tropopause dip, and so passes through stratospheric air of lower PV than the 250hPa level.

The relation between this PV structure and the WV image is an illustration of Demirtas' rule no. 1. This type of PV-WV image relation is always seen in relation to cyclonic development. However, rule no. 1 as given by Demirtas is somewhat unclear. It appears that there are *two* distinct maxima within this type of PV structure - the one associated with the tropopause dip, which is usually dominant at the 250/300hPa levels; and the one associated with the dry intrusion circulating around the tropopause dip, which is usually more prominent at the 400/450 hPa levels. The first PV maximum generally occurs in a 'pivot point' disposition relative to the dry intrusion; the second is generally colocated with the brightest part of the dry intrusion itself.

It is puzzling that the 250hPa PV maximum appears to coincide with a relatively moist part of the image, rather than a dry feature, as might be expected. Numerous other examples of this sort of arrangement have been seen in the cases examined so far. A possible (but not entirely satisfactory) explanation may be that either there is a layer of cloud just below the tropopause at this point, so that the WV image appears relatively moist at this location, or else the dry air at the centre of the tropopause dip has become mixed with moister tropospheric air.

Dry feature no.2

The elongated dry intrusion feature located along the western side of the WV image is associated with a complex area of high PV. At 250hPa, a very sharp PV gradient follows the western edge of the dry intrusion. A less sharp PV gradient follows the edge of the moist region to the east of the dry intrusion. These seem to be in accordance with Demirtas' rule no.2. Such PV gradients presumably indicate the lines of intersection between the tropopause and the isobaric (or isentropic) level on which the PV contours are plotted.

A number of PV maxima occur within this high PV complex on 250hPa. It is difficult to disentangle their relation to the WV image, although the roughly circular PV maximum located just above the southern edge of the image is apparently located within the dry intrusion. This may represent a tropopause dip.

At 400hPa the structure of the high PV region is somewhat simpler. There is a pair of twin PV maxima just above the southern edge of the image, within a bright region of the dry intrusion feature, and an elongated PV maximum within the more northerly part of the dry intrusion. These probably represent the PV signature of the dry intrusion air itself.

Dry feature no.3

This dry intrusion feature is located below intrusion no.1, at the bottom of the image. The eastern end of this feature has a local PV maximum lying within it on 250hPa, and at 400hPa there is a local PV maximum at the western end. These are probably the signatures of a stratospheric intrusion.

Dry feature no.4

This is located in the NE corner of the image. It has a region of high PV gradient running through it on both the 250 & 400hPa plots. The 300 & 500hPa height plots show that this dry feature is at the base of an upper trough, so it could be considered as an illustration of Demirtas' rule no.3.

3.1.2 Situations in which the PV - WV Image Relation breaks down

The high BT features considered above are all clearly related to cyclonic systems. However, features in the yellow-red range are often seen on WV images which are not so related. The PV - WV relation which this project is attempting to define is valid only in the vicinity of the jet stream. There are various types of circumstance in which high BT features which appear on the WV image are not associated with high PV, or in which the "principles" of the PV - WV relation cannot be readily applied.

Regions of anticyclonic descent appear as high BT regions, simply because adiabatic descent warms up and dries out the air. In such regions, as in dry intrusion regions, the satellite sees further down into the atmosphere than in moist or cloudy regions, and so the radiation recieved has a higher BT. However, such regions are not associated with high PV at upper tropospheric levels, but rather with low PV.

Confusion may be caused by dry air becoming mixed with moist air in older cyclonic systems, or by cloud overlying dry intrusions. Relatively high PV may be generated at low tropospheric levels either diabatically or by intense cyclonic circulation, as in tropical storms. Such high PV regions may reach fairly high levels in the troposphere, but would tend to be associated with moist air rather than dry.

3.2 Approaches to PV Adjustment

The issue of how to make appropriate adjustments to model-derived initial PV fields has been approached in a number of ways, some of which use WV imagery and some of which do not. Some of these approaches have been tried out in case studies, and all of these have a manual element. This section gives a brief account of all the possible approaches to PV adjustment in this project which have been considered or actually tried in practice, and also discusses some of the issues and uncertainties relating to PV adjustment which some of these approaches attempt to address.

3.2.1 Direct Use of the PV / WV Image Comparison

In the formulation of this project, the comparison between upper-tropospheric PV fields and WV images was envisaged as the principal means by which "detection of analysis errors" and "correction of errors" would be carried out. Attempts have been made in a number of case studies to utilise whatever "guidance" this comparison provides to adjust the initial PV field at U-T levels (see chapter 2 of this report for some of the technical details). Such adjustments have been made in a number of ways:

(a) by displacing PV elements from their original location to another location which is considered to provide a better "fit" with WV image;
(b) by scaling PV elements without displacing them;
(c) by displacing and scaling PV elements simultaneously;
(d) by "erasing" part of a PV field which was considerd to be "mismatched" with the WV image, and reconstructing it manually in such a way that it "matched" the PV field.

Many of the attempts to use these procedures in the earlier stages of this project are now considered to have been misguided, as they were based on certain misconceptions regarding the PV/WV image relation. In fact the only attempts which have given any positive impact as yet are those which involved scaling without significant displacement. All these adjustments have been arrived at on a trial-and-error basis, as there is as yet no well-defined mathematical or statistical relation between PV fields and WV images.

3.2.2 The Use of WV Images and Pseudo WV Images as "Substitute PV Fields"

This approach is based on the assumption that there is a simple 1-1 correspondence between features of the WV image in the jet stream vicinity, and features of the PV

field at upper tropospheric levels, i.e., it is assumed that the U-T PV fields should look similar in their structure to the WV image. This assumption is now considered to be completely erronious, but at an earlier stage of the project it was thought to be valid and so was used as basis for PV adjustment in some case studies. The cases in which this approach was used gave a negative impact on the forecast (cases 1 & 3, see chapter 5).

The procedure was as follows.

(a) The U-T PV fields are compared with the WV image to determine which part of the PV field should be adjusted, and which part of the WV image corresponds to it.

(b) The brightness temperature field of the WV image is converted to PV units by simple scaling. The notional scaling factor is arrived at by comparing the range of brightness temperature in the image, in K, with the range of the PV field on any given level, in PV units. Different scaling factors would be appropriate for different vertical levels in the atmosphere. Scaling factors are determined for all the pressure levels on which adjustment is to be carried out. The WV image data may be on a grid of higher resolution than the UM grid, if so the resolution of the image data would have to be reduced to that of the UM grid.

(c) The relevant portion of the model PV field, at each of the pressure levels involved, is overwritten with the corresponding portion of the "substitute" PV field derived from the WV image. Additional adjustments may be made around the edges of the overwritten portion to reduce the inevitable discontinuities which arise.

In a couple of cases (case 9, rerun 1 & case 14, rerun 4; both gave negative impacts - see chapter 5) this sort of procedure was carried out with a "pseudo" WV image rather than the satellite WV image. A pseudo image is generated by a radiation transfer algorithm which attempts to compute a radiance field at a given wavelength from model-derived vertical temperature and humidity profiles. The algorithm used in this work was the Schmetz scheme without cloud effects (Schmetz and van de Berg 1994). It has been found that, in general, such pseudo images bear some resemblance to the corresponding satellite image, albeit with much less detailed structure. It should be noted that cloud effects make an important contribution to the satellite WV image, so their absence from the pseudo image is a serious deficiency. WV imagery with cloud effects is not as yet available to this project.

3.2.3 The Inspection of PV Error Fields

This approach to PV adjustment does not involve WV imagery. It was partly suggested by the work of Fehlmann et al. on PV retrodiction (Fehlmann 1997, Fehlmann and Davies 1997). Their approach involves computing the difference between a forecast PV field and an analysed PV field to give a PV error field. The PV error elements are then "advected" backwards in time in 6-hourly steps, with PV inversion at each stage, to determine a revised initial state for the forecast.

The facility to carry out PV retrodiction is not available to this project, nor is it considered appropriate for the context of this work. However, it was considered that the inspection of PV error fields for a T+6 forecast may shed some light on the PV adjustments which are required at T+0. By examining the difference between the forecast and analysed fields for a time 6 hours after the start of the forecast, one can determine where errors in the PV field begin to develop. The initial PV field can then

be adjusted accordingly at these locations, in the hope that this will improve the initial state of the forecast. One advantage of this approach is that it can be carried out on any vertical level in the atmosphere, and so allows for PV adjustment at lower tropospheric levels as well as upper levels.

This technique was attempted in only one case, namely case 11 in chapter 5. PV adjustments were made on a number of tropospheric levels from 850hPa to 450hPa, based on the inspection of PV error development at T+6. There was no significant impact on forecast development, however. (It was subsequently found for this particular case that upper tropospheric adjustment alone was able to yield an improved forecast). In spite of this negative result, the "PV error fields" approach should at least be of some use to indicate which elements of a PV field are precursors of error development.

3.2.4 Lower Tropospheric PV Adjustment

In some of the case studies (reported in chapter 5) it has been found that a positive impact on the forecast surface pressure development of a cyclone can be obtained by scaling an appropriate upper-tropospheric PV element. However, this may not lead to a positive impact on the forecast of, say, geopotential height or temperature at mid- or upper-tropospheric levels, and may even have a negative impact. In other cases, particularly the Christmas Eve '97 case (case study 14 in chapter 5), no positive impact on surface forecast development has been achieved with any of the upper-tropospheric PV adjustments which have been attempted. This may suggest that lower-tropospheric PV adjustment should also be considered.

It may be that upper-tropospheric PV elements located on a particular isentropic surface interact with lower tropospheric PV elements on the same isentropic surface, a view which finds support in Feldmann and Davies (1997). If upper tropospheric adjustment is carried out without lower level adjustment, this may be detrimental to such phase relations. In some cases it may be that the surface forecast is actually insensitve to upper-tropospheric PV adjustment, whereas it can be affected by lower tropospheric adjustment (see, for example, Demirtas 1996).

Even in cases where upper-tropospheric adjustment is of primary importance, the PV adjustments need to be carried out on a range of pressure levels, which may extend down towards lower tropospheric levels. A WV image only provides guidance about PV adjustment on a single 2-d surface. Ideally, some sort of guidance is required which would enable adjustments at a lower level to be determined, and then adjustments at other levels could perhaps be obtained by interpolation. There may be some surface or near-surface observation types which could be helpful, eg. scatterometry data on low-level winds.

The issue of low-level PV analysis is probably of considerable importance in a broader sense. In general, it is important to understand the evolution of weather systems (both forecast and actual systems) in three dimensions, throughout the depth of the troposphere, in order to appreciate the role played by both upper- and lower-level forcing. If such a complete picture could be arrived at, then perhaps it would be possible to postulate PV adjustments throughout the depth of the troposphere which would improve forecast development. It is strongly suspected that such a complete understanding would be important in the Christmas Eve 97 case (case 14 in chapter 5), for example. Conceptual models of cyclogenesis (Semple 1998) may be helpful in this regard, although it must be borne in mind that they provide only qualitative guidance.

3.2.5 The possibility of using total ozone data

Numerical experiments with total ozone data have indicated that total ozone is correlated with the pressure-weighted average PV over an appropriately chosen depth of upper troposphere and lower stratosphere (Li 1998). It therefore seemed of interest to consider whether total ozone data could be useful in this project, as a supplement to WV imagery.

The availability of total ozone data was therefore investigated. There is only one source for this data, namely NASA. The NASA data is obtained by the 'Earth Probe' Total Ozone Mapping Spectrometer satellite. Unfortunately, it emerged that this data is not useful for the purposes of this project. The satellite is in fact a polar orbiting satellite, which covers the entire globe every 24 hours. The ozone measurements are taken in sequence as the satellite orbits, each measurement covering a small domain directly below the satellite. Thus, each part of the globe is covered once in 24 hours. To be useful for this project, the data would have to be in the form of a contemporaneous image covering the entire N Atlantic area (like the Meteosat WV images), and would have to be available at least every six hours. It would also have to have a somewhat higher resolution than is currently available from Earth Probe. The current resolution is no better than 1 degree square.

It was therefore decided that total ozone data in its present form is not useful for this project, and is not worth investigating further. A more useful form of total ozone data may be available in the future, from the Meteosat Second Generation satellite.

3.3 Possibilities for Automated PV Adjustment

In the case studies which are being pursued as part of this project, adjustments are made to initial PV fields using an essentially manual technique, based on qualitative judgement. As has been emphasised already, it is vital to establish a precise quantitative relation between upper tropospheric PV fields and WV images, and to utilise this in an automated computational system for the optimal adjustment of PV fields. Two possible solutions to this problem are being pursued in conjunction with this project.

R.N. Hoffman of AER inc., is proposing to use the "Distortion Representation" approach (Hoffmann et al., 1995) to align a pseudo WV image with the corresponding satellite WV image. The "displacement field" derived from this procedure would then be applied to the corresponding PV field on an upper-tropospheric pressure surface, so aligning the PV field with the satellite WV image.

The pseudo WV image is derived from model-generated temperature and humidity profiles via a radiation-transfer algorithm (such as the Schmetz scheme, Schmetz and van de Berg, 1994). The Hoffman approach seems to assume that the pseudo WV image corresponds, in the disposition of its features, to the model's upper-tropospheric PV fields. Actual inspection of pseudo WV images indicates, however, that this assumption is questionable. In general, pseudo WV images do not appear to correspond to the model's U-T PV fields. In fact, they tend to resemble the satellite WV image as far as gross features are concerned. Furthermore, the notion that the

U-T PV fields, or portions of them, should be *aligned* with WV image features (a view which a number of authors seem to hold, as has been noted already) may not be generally appropriate. However, it may be that displacements can be derived relating smaller features of the satellite and pseudo WV images, which it would be appropriate to apply to corresponding PV elements.

An alternative technique is being investigated by G. Pankiewicz of the UK Met. Office. This involves trying to infer the PV field, on an U-T isentropic surface, from the WV image, using a pattern recognition system which has been 'trained' in the PV-WV relation by processing large numbers of WV images, and their corresponding PV fields on a suitable isentropic surface. This approach seems more promising a priori; but its success depends on an adequate level of correlation between the PV and WV training data sets.

It should be noted that both of these approaches are two-dimensional; neither could provide any guidance on the significant question of how a PV adjustment field should vary from level to level in the vertical.

Figures for chapter 3

Fig. 3.1 PMSL analysis, 6z 20/10/97

Fig. 3.2 Background WV image 6z 20/10/97; Contours PV on 250hPa
Range 0-12 PVU, Interval 1 PVU

Fig. 3.3 Background WV image 6z 20/10/97, Contours PV on 400hPa
Range 0-5 PVU, Interval 1 PVU

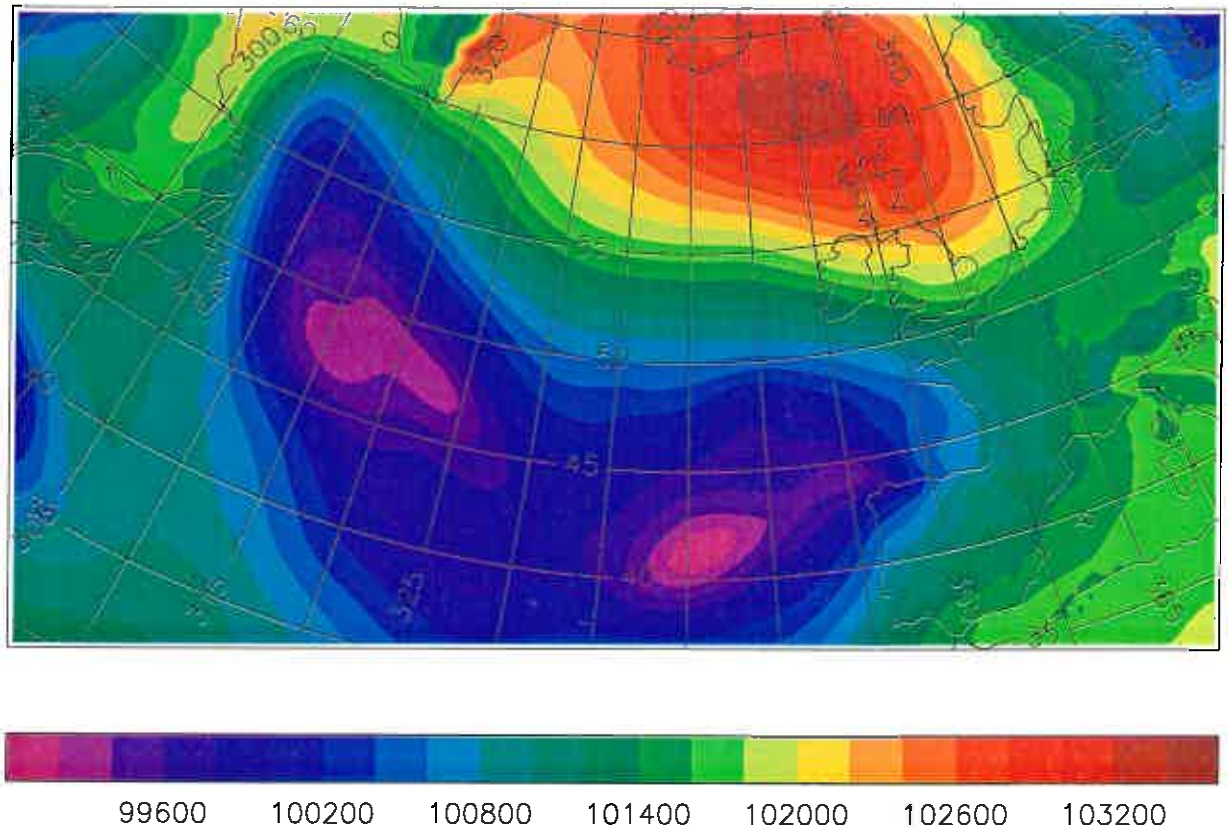
99600
100200
100800
101400
102000
102600
103200

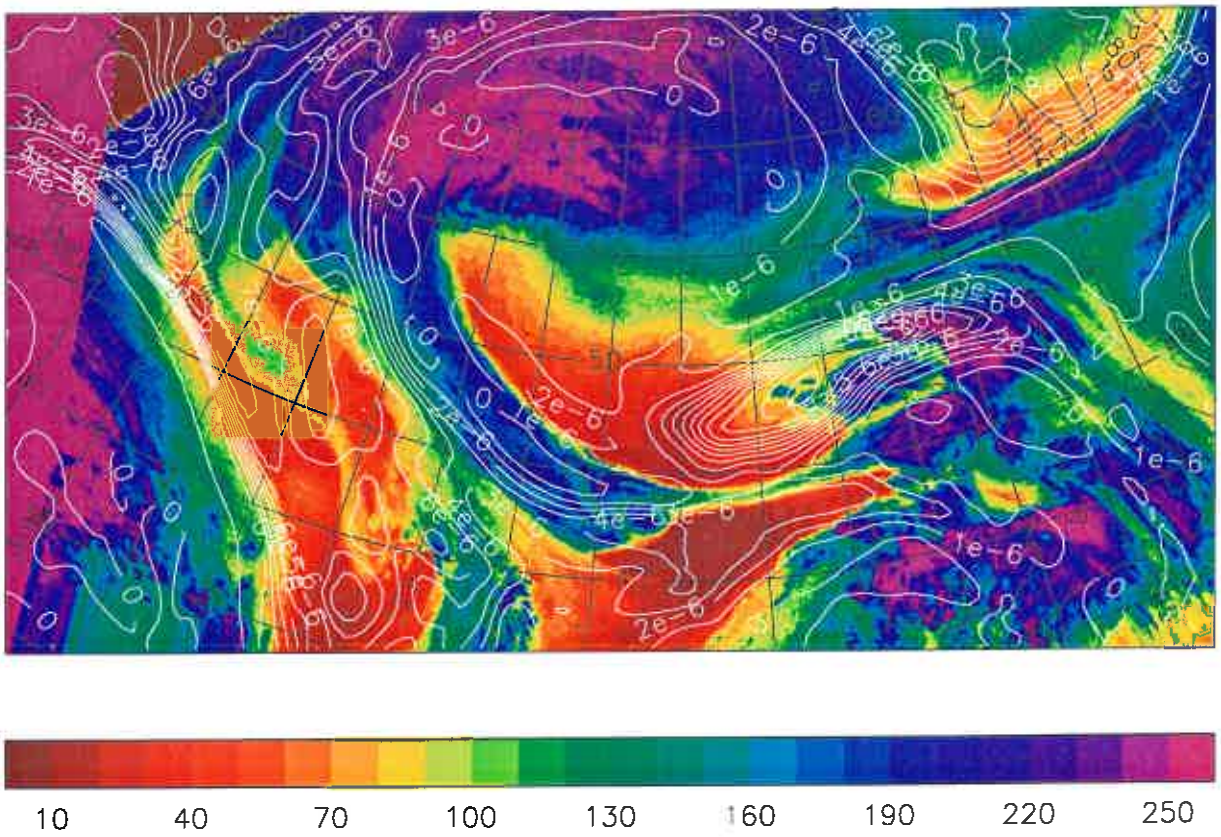
10
40
70
100
130
160
190
220
250

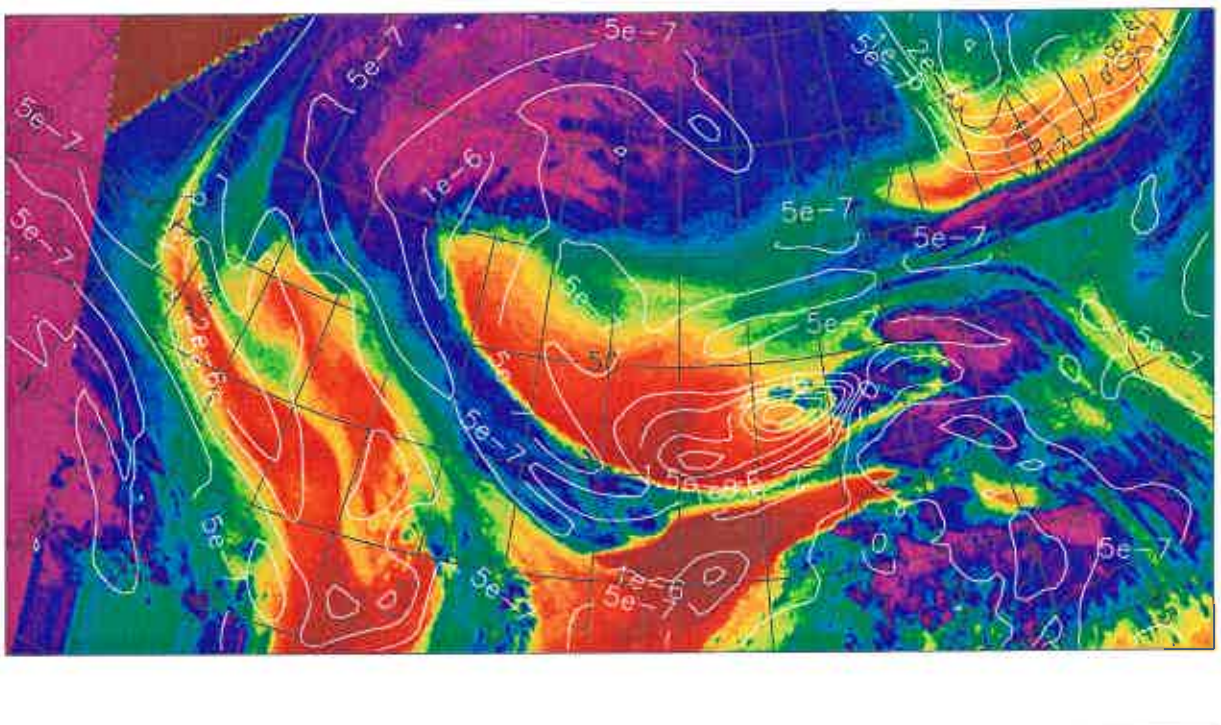
10
40
70
100
130
160
190
220
250

4. THE PV INVERSION TECHNIQUE

This chapter gives a brief account of the PV inversion program used, and an account of the undesirable features of it which impact on this work. More details of the PV inversion scheme can be found in Ziemanski (1994), Demirtas (1996), Griffiths et al. (1998) and Davis and Emanuel (1991).

4.1 The PV Inversion Program

4.1.1 Governing Equations

The PV inversion program used in this project was derived from a program developed by M Ziemanski (Ziemanski, 1994), and modified by M Griffiths (Griffiths et al., 1998). The basis of the PV inversion algorithm is as follows.

The definition of Ertel PV is

$$q = \frac{1}{\rho}\vec{\eta}\cdot\nabla\theta \tag{1}$$

where ρ =density, $\vec{\eta}$ = absolute vorticity vector (relative vorticity + planetary vorticity f), θ =potential temperature. The form (1) is appropriate when the vertical coordinate is height; if pressure is used as vertical coordinate, the $1/\rho$ factor does not appear. Equation (1) may be expressed approximately in terms of the geopotential Φ and stream function Ψ,

$$q = \frac{g\gamma\pi}{p}\left[\left(f+\nabla^2\Psi\right)\Phi_{\pi\pi} - \frac{1}{a^2\cos^2\phi}\Psi_{\lambda\pi}\Phi_{\lambda\pi} - \frac{1}{a^2}\Psi_{\phi\pi}\Phi_{\phi\pi}\right] \tag{2}$$

where λ,ϕ =longitude, latitude; π =Exner pressure (the vertical coordinate), a=Earth radius, g=acceleration due to gravity, $\gamma = R_d / c_p$, p=pressure, f=Coriolis parameter. The approximations made in transforming (1) into (2) are
(a) the hydrostatic approximation, i.e. derivatives of vertical velocity are neglected;
(b) horizontal velocity is expressed in terms of the stream function Ψ, which implies that it has zero divergence:

$$u = -\partial\Psi/\partial y\ , \quad v = \partial\Psi/\partial x \tag{3}$$

where x, y are the local horizontal coordinates in the eastward, northward directions. Equation (2) is a Poisson-like elliptic equation. Given a set of PV fields q on pressure levels, we wish to solve this equation for the Ψ,Φ fields. To form a complete system we need another equation relating Ψ,Φ, i.e., a balance condition. Various balance conditions are possible; the one used in this algorithm, following Davis and Emanuel (1991), is the Charney non-linear balance condition, which may be expressed in terms of Φ,Ψ as follows:

$$\nabla^2\Phi = \nabla\cdot\left(f\nabla\Psi\right) + \frac{2}{a^4\cos^2\phi}\left(\Psi_{\lambda\lambda}\Psi_{\phi\phi} - \Psi_{\lambda\phi}^2\right) \tag{4}$$

This is essentially a generalisation of gradient wind balance, i.e. it includes forces arising from the curvature of air parcel trajectories.

Equations (2), (4) form a complete system for Ψ,Φ. The balance equation (4) is two-dimensional, whereas the PV equation (2) is three-dimensional. Equation (4) is rearranged somewhat:

$$\nabla^2\Psi = \frac{1}{f}\left[\nabla^2\Phi - \frac{1}{a}\beta\Psi_\phi - \frac{2}{a^4\cos^2\phi}\left(\Psi_{\lambda\lambda}\Psi_{\phi\phi} - \Psi_{\lambda\phi}^2\right)\right] \tag{5}$$

where $\beta = df/dy$.

In the PV inversion algorithm employed by this project (Ziemanski 1994, Griffiths 1998), equation (2) is replaced by a linear combination of (2) and (4); since they have different units, equation (2) is multiplied by a scaling factor c,

$$c = \left(H^2 / fL^2\right)\left(g/\theta_0\right)^2$$

where H, L are characteristic horizontal and vertical length scales, and $\theta_0 = 300K$ is a reference temperature. The resulting equation is

$$\begin{aligned}\nabla^2\Phi + c\left(f + \nabla^2\Psi\right)\Phi_{\pi\pi} &= \frac{p}{g\gamma\pi}cq + c\left[\frac{1}{a^2\cos^2\phi}\Psi_{\lambda\pi}\Phi_{\lambda\pi} + \frac{1}{a^2}\Psi_{\phi\pi}\Phi_{\phi\pi}\right] \\ &+\nabla\cdot\left(f\nabla\Psi\right) + \frac{2}{a^4\cos^2\phi}\left(\Psi_{\lambda\lambda}\Psi_{\phi\phi} - \Psi_{\phi\lambda}^2\right)\end{aligned} \tag{6}$$

The values for H, L which give the best convergence rate are 10km and 2000km. In the PV inverter, the 2-d balance equation (5) and the 3-d PV equation (6) are solved for Φ,Ψ in a system of iterative loops. The balance equation (5) is solved iteratively for the Ψ fields, given a set of Φ fields; and the PV equation (6) is solved iteratively for the Φ fields, given a set of Ψ fields. Both of these iterative procedures employ successive under-relaxation to assist convergence. As the solution approaches convergence, the PV fields recalculated from Φ,Ψ on each iteration should approach the input PV fields. The convergence criteria may be based on the fractional change in Φ or Ψ from one iteration to the next, or on the difference between the input PV fields and the recalculated PV fields. In practice, any two of these three criteria are used, and the convergence threshold is set according to how accurate a solution is required. In general, a compromise is made between accuracy and computation time.

A consequence of the approximation (b) above, i.e. the assumption of zero divergence for the wind field, is that the wind field computed from the PV inverter's output fields is also non-divergent - the divergent part of the wind field is not recovered.

4.1.2 PV Inversion Domain and Input Fields

The PV fields input to the inverter are derived from a set of UM analysis fields or background fields. The PV is generally computed by the UM and then input to the inverter, although the inverter itself could compute the initial PV fields from the input

UM geopotential, wind velocity, and potential temperature fields. The PV fields computed by the inverter differ slightly from those computed by the UM, although this difference is virtually insignificant in practice.

The horizontal PV inversion domain is a subset of the UM (LAM or global) domain. The vertical levels are pressure levels, since the PV inversion algorithm is formulated on (exner) pressure levels. The range of levels used is generally 800hPa to 50hPa, with an interval of 50hPa. The horizontal domain is limited by the need to avoid orography, since PV is undefined below ground level; in the N Atlantic this implies that the domain cannot extend further north than the southern tip of Greenland, unless the bottom boundary is raised to 600hPa. A bottom boundary of 800hPa does allow the domain to encroach to some extent on western Canada without encountering orography.

4.1.3 Boundary Conditions

The boundary condition used for the 2-d balance equation (5) is to specify Ψ on the boundary. It must be specified in such a way that the tangential derivative $\partial\Psi/\partial s$ matches the normal wind component, to be consistent with eq. (3); and also so that the divergence of the velocity through the boundary is zero, i.e., the integral of $\partial\Psi/\partial s$ around the boundary must vanish. (In other words, Ψ satisfies the planar version of Green's theorem). This can be achieved if the value of Ψ on the boundary is specified by (Davis and Emanuel 1991),

$$\frac{\partial\Psi}{\partial s} = -\vec{v}\cdot\vec{n} + \frac{\oint \vec{v}\cdot\vec{n}\,dl}{\oint dl}$$

If Ψ is specified at one point on the boundary, then it is determined at all boundary points by this condition.

The boundary conditions for solving the 3-d PV equation (6) are also as in Davis and Emanuel (1991). On lateral edges, the value of Φ is taken from the input UM fields. On the top and bottom horizontal boundaries (usually at 50mb and 800mb), the hydrostatic balance condition is used, in the form $\Phi_\pi = -\theta$, where potential temperature θ is taken from the input UM fields. Alternatively we could specify the value of Φ rather than its vertical derivative; according to Davis and Emanuel (1991) the solutions are fairly insensitve to the choice of horizontal boundary condition.

4.2 Difficulties with the PV Inversion Technique

4.2.1 The divergent component of the wind fields and the balance assumption

As noted above, the wind fields computed from the PV inverter's output fields are non-divergent, because of the approximations made in the PV inversion algorithm. It is therefore not desirable to use these wind fields directly for input to the UM, as the divergent component of the wind fields would be lost. Instead, the wind adjustments are input as increments to the UM initial wind fields. This involves carrying out two PV inversions, one on the adjusted PV fields, and one on the original PV fields (see chapter 2). Such a differencing procedure is not strictly valid, in view of the highly non-linear nature of the PV inversion algorithm, but it is nonetheless required for the reasons stated here, and for other reasons (eg. the fact that the PV inversion is not

carried out on UM model levels, which may also lead to loss of information). It seems reasonable to suppose that such differencing is acceptable as long as the wind adjustments are not too large.

A further inconsistency is introduced by the fact that the PV inverter assumes the Charney non-linear balance condition, which is not the same as the balance condition used by the UM dynamics scheme. However, this inconsistency is judged to be within acceptable limits. It has been commented that the assumption of *any* balance condition may be inappropriate, in that the regions in which PV adjustment is most likely to be applied are the very regions in which the flow is most likely to be unbalanced. The balance assumption excludes the possibility of gravity waves, which may be significant in these regions.

4.2.2 The need for vertical interpolation

The fact that the PV inversion is carried out on pressure levels implies that the output winds and temperatures are also computed on pressure levels. Before they can be used for the adjustment of UM input fields, they have to be interpolated onto UM model levels. This is not difficult, but it does introduce yet another stage of approximation.

4.2.3 The lower boundary condition and surface pressure adjustment

As explained above, the bottom boundary condition used in the PV inversion algorithm is to specify the θ field. Φ is not fixed on this boundary, and so will be changed by the PV inversion process. As the bottom boundary is a pressure level it cannot be coincident with the earth's surface, which forms the bottom boundary in the UM. This implies that compensating adjustments should be made to the surface pressure, and to the geopotential heights of all pressure levels between the earth's surface and the PV inverter's bottom boundary (and, consequently, to the corresponding wind and temperature fields). These adjustments have not been made in fact. Their computation would present some significant difficulty. If the alternative bottom boundary condition was used, i.e. to specify Φ and allow θ to vary, compensating adjustments would still be required as this would also change surface pressure.

Some attempt has been made to judge the magnitude of the effects caused by this inconsistency. A 24 hour surface pressure animation was created for one particular case study, in order to reveal in a subjective manner the extent of any spurious oscillations which result. It was found that these oscillations were visible for the first six hours, but not visible thereafter. The order of magnitude of the maximum amplitude of the oscillations amounted to about 10% of the pressure adjustment resulting from the PV inversion. As the time scale of these oscillations was limited, it was felt that their effect on case study results on time scales of 12-36 hours could be discounted.

This is clearly not a totally satisfactory situation. However, the best solution to this problem would be a PV inverter based on UM model levels rather than pressure levels; it would then be possible to have a PV inversion domain whose bottom boundary was at the earth's surface, so the surface inconsistency problem would not arise. As there are also other reasons for wishing to develop such a PV inverter, it would not seem worthwhile to expend significant effort on the development of a separate adjustment algorithm to overcome the inconsistency problem, but rather to direct effort to the development of an improved PV inverter.

4.2.4 Covergence Difficulties

The PV inverter sometimes fails to converge for a particular set of PV fields. In some cases the failure is very sudden, i.e. the values of the error parameters become very large on a particular iteration, after having been steadily decreasing over a number of previous iterations. In other cases, the failure is very gradual and the error parameters may simply maintain more or less constant large values over many iterations without any tendency to reduce.

Such failures often appear to be associated with a very sharp gradient in the PV field; if the solution domain is reduced so that the troublesome locality is excluded, then convergence will be achieved, although the excluded part of the field may in fact encompass the very PV anomaly which the particular case study is focusing upon. (It may be that the problem in such cases arises not from the sharpness of the gradient, but from the existence of negative PV values at such locations).

If the convergence failure is gradual, then it may be acceptable to relax the convergence limits, and still achieve a sufficiently accurate converged solution.

4.2.5 Domain Edge Effects

Since the PV inversion domain is a subset of the UM domain, there are always discontinuities at the horizontal domain boundary edge, between the adjusted wind (or temperature) field, and the remainder of the UM field into which the adjusted field portion has been inserted. However these discontinuities do not appear to have a significant effect on the UM, and are smoothed out in the first few timesteps. Their effect appears to be much less than that of the inconsistencies caused by the lower horizontal boundary condition, for example.

5. OVERVIEW OF CASE STUDIES

A total of 14 cases have been studied so far, and for most of these several reruns were carried out. All of them utilised the UM vn4.3 LAM on the T3E. Of the 14 cases, 10 were from Autumn 1997, mostly separated by seven day intervals. 3 cases were from the FASTEX period (Feb. 97) and the remaining case was the Christmas Eve 97 storm.

There has been considerable variation in the approaches taken to PV analysis and PV adjustment among these cases. The main reason for this is that the author's understanding of the relation between upper tropospheric PV fields and water vapour images has evolved over time. However, a greater degree of uniformity of approach has developed in the more recent case studies, as earlier misconceptions regarding the PV/WV relation have been discarded.

Some sort of positive impact on surface pressure development was obtained in six of the fourteen cases - cases 2,4,6,7,11 & 13. Of these, 4,6 & 11 gave significant positive impacts, the rest gave small impacts. Case 8 gave a mixed impact on surface development (i.e., positive in some respects, negative in others). In some of the later cases, impact at 500hPa was also examined; case 13 gave a positive impact at the surface, but a negative impact aloft. The only means used to judge "impact" so far has been subjective analysis of plotted fields.

The technical limitations of the case studies should be borne in mind, particularly the crudity of the manual PV adjustments and the limitations of the PV inverter with regard to restricted solution domain and convergence failure.

What follows is, in section 5.1, a very concise summary of all 14 cases, followed by section 5.2 which contains more detailed accounts. Cases 4, 6 & 11 are illustrated by coloured graphics (these are probably the most interesting cases). The other cases are not accompanied by graphics. This is unfortunate but the cost of colour reproduction is prohibitive. Monochrome reproduction of the graphics is very unsatisfactory.

5.1 Concise Summary of Cases

In all reruns, except for rerun 2 in case 3, the rerun forecast started from an adjusted UM analysis, with no assimilation. Rerun 2 in case 3 started from adjusted background fields.

Each concise summary gives: (a) the nature of the error in the forecast which the case study attempts to address; (b) the type of PV adjustments employed, and the outcome of the rerun forecasts. For explanations of the PV adjustment techniques, see chapters 2 & 3 of this report.

All the PV adjustments referred to were carried out at upper tropospheric levels, i.e. in the range 250 - 500hPa. Lower level PV adjustments were attempted case 11, but with no significant impact.

Case 1 Small negative impact

Forecast duration: 6z 3/2/97 - 0z 5/2/97 (FASTEX IOP 10)

Type of forecast error: Position error in a ridge - forecast position too far W.
Rerun forecasts: 2 reruns. WV image used as substitute PV. Small negative impact on surface pressure.

Case 2 Small positive impact

Forecast duration: 0z 8/2/97 - 12z 9/2/97 (FASTEX IOP 11a)

Type of forecast error: Cyclone under developed, slight position error.
Rerun forecasts: 4 reruns. PV anomaly erased, and reconstructed in a displaced location. Small positive impact on intensity in rerun 4 (with most intense PV).

Case 3 Small negative impact

Forecast duration: 0z 9/2/97 - 0z 10/2/97 (FASTEX IOP 12)

Type of forecast error: Cyclone under developed, no positon error.
Rerun forecast: WV image used as substitute PV. Small negative impact on surface pressure.

Case 4 Significant positive impact

Forecast duration: 12z 1/9/97 - 12z 3/9/97

Type of forecast error: Cyclone under developed, slight position error.
Rerun forecasts: 3 reruns. PV anomaly scaled up & extended downwards. Slight horizontal displacement. Positive impact on surface pressure in rerun 3.

Case 5 Null case

Forecast duration: 12z 8/9/97 - 12z 10/9/97

This case was wholly anticyclonic within the PV inversion domain, and offered no scope at all for PV adjustment (there were no PV anomalies within PVI domain).

Case 6 Significant positive impact

Forecast duration: 12z 15/9/97 - 12z 17/9/97

Type of forecast error: Cyclone decayed too rapidly, no position error.
Rerun forecasts: 2 reruns. Rerun 1, PV anomaly scaled up and displaced. Rerun 2, PV anomaly scaled without displacement. Positive impact on surface pressure, RR1 had about twice the impact of RR2.

Case 7 Small positive impact

Forecast duration: 12z 22/9/97 - 12z 24/9/97

Type of forecast error: Cyclone 1 decayed too rapidly, cyclone 2 under developed. No position errors.
Rerun forecasts: 3 reruns. RR1 & RR2 focused on cyclone 1. PV anomaly scaled up and extended downwards. Mixed effect on surface development.
RR3 focused on cyclone 2. PV anomaly scaled up. Small positive impact on surface development.

Case 8 Mixed impact

Forecast duration: 12z 29/9/97 - 12z 1/10/97

Type of forecast error: Cyclone decayed too rapidly.
Rerun forecast: PV anomaly scaled up. Cyclone deepened, but too much. Mixed impact on surface development.

Case 9 Negligible impact

Forecast duration: 12z 6/10/97 - 12z 8/10/97

Type of forecast error: Multiple cyclonic development with large position and intensity errors.
Rerun forecasts: 3 reruns. RR1 - WV image used as substitute PV. Negative impact on surface pressure development.
RR2 - PV anomaly displaced. No impact on surface development.
RR3 - PV anomaly scaled up without displacement . Slight positive impact on surface development.

Case 10 Negligible impact

Forecast duration: 6z 7/10/97 - 6z 9/10/97

Type of forecast error: Some error in position and intensity of cyclone at T+36, otherwise no significant error.
Rerun forecasts: Anomaly scaled down, attempt to improve T+36 forecast. No impact on surface development.

Case 11 Significant positive impact

Forecast duration: 6z 13/10/97 - 6z 14/10/97

Type of forecast error: Cyclone under developed, no position error.
Rerun forecasts: 3 reruns, PV anomalies scaled up. Positive impact on surface development. Slight positive imapct at 500hPa.

Case 12 Null case

Forecast duration: 6z 20/10/97 - 6z 21/10/97

There was no significant error in this forecast. No reruns were attempted. As a very good forecast, this case is useful for what can be learned about the PV - WV image comparison - see chapter 3 for a discussion of this.

Case 13 Small positive impact at surface (small negative impact aloft)

Forecast duration: 6z 27/10/97 - 6z 28/10/97

Type of forecast error: Cyclone decay started several hours too late.
Rerun forecast: PV anomaly scaled down. Positive impact on surface development, negative imapct at 500hPa.

Case 14 Negative impact

Forecast duration: 6z 23/12/97 - 6z 25/12/97 (CE Storm 97)

Type of forecast error: Rapid cyclonic development with gross position and intensity errors.
Rerun forecasts: 5 reruns attempted. Reruns 1,2,3 & 5 involved displacement and scaling of PV anomalies. These gave negligible impact on surface development. Rerun 4 used the pseudo WV image as substitute PV. This gave a large negative impact on surface development.

5.2 Detailed accounts of case studies

Most of the case study accounts have the following structure:
(a) An account of the original forecast and the errors which developed within it;
(b) A brief description of the WV image at the initial forecast time and how it compared with the upper-level PV fields;
(c) An explanation of the PV modifications which were made;
(d) The impact which the PV modifications had on the forecast.

CASE 1. 6Z 3/2/97 TO 0Z 5/2/97 IOP10

Original Forecast

In the analyses, a ridge moved from mid-Atlantic to a location over the UK at 0z 5/2/97, weakening fairly significantly as it did so. In the original LAM forecast, the ridge moved too quickly eastward, so that at 0z 5/2/97 (T+36) it was located over the North Sea. The weakening was less advanced than in the analysis. At T+36 the forecast had developed a weak trough over the UK.

WV Image and PV Fields

The WV image at 6z 3/2/97 showed a zonally-elongated dry feature apparently corresponding in position and distribution with the ridge referred to above. The upper troposheric PV fields (eg. at 300hPa) showed a large complex region of high PV over the NW Atlantic. A zonally-elongated PV anomaly on the southern edge of this region was clearly associated with the above dry feature. It had a PV maximum of 6 units. The dry feature was distributed over the southern flank of this anomaly. The PV anomaly was probably associated with the decay of the ridge referred to above.

PV Adjustments

At this early stage of the project it was thought (erroniously) that a 1-1 superposition relation between the WV image and the upper tropospheric PV distribution should exist in the vicinity of the jet stream. The observation that the brightest part of the dry region was not colocated with the maximum of the PV anomaly, but actually lay slightly south of it, was considered to represent a 'mismatch'. The objective of the PV adjustments which were performed was to 'correct' this 'mismatch'.

Two reruns were carried out. In both cases the real WV image was used as a substitute PV field in the region of interest. The WV brightness temperature field was 'converted' to PV units by simple scaling, the scaling factor having been estimated from the WV/PV comparison. A small portion of this field encompassing the relevant dry feature was 'pasted' into the analysed UM PV field. This procedure was carried out on pressure levels 300,350,400 & 450hPa, with a different conversion scaling factor for each level. In rerun 1 the western half of the pasted portion on each level was scaled down (to reduce the total amount of PV in the pasted portion), whereas in rerun 2 the pasted portion was unaltered.

Results

In both cases the surface pressure forecast was made slightly worse. The position error in the eastward moving ridge was not corrected, and there was a tendency for the weak trough over the UK at T+36 to develop into an actual cyclone. This tendency was greater in rerun 2.

It is now considered that the 'cut & paste' approach used in this case is invalid, since it is based on a false view of the PV/wv image relation. Furthermore, the relation between the PV anomaly and the dry feature does not in fact clearly represent a mismatch, as was previously thought. It is interesting, however, that adjustment of this PV anomaly had a marked effect on the cyclonic development occurring W of the ridge, while it had no effect on the position error of the ridge itself.

CASE 2. 0Z 8/2/97 TO 12Z 9/2/97 IOP11A

Original Forecast

In the analyses, a mid-Atlantic trough developed into a compact cyclone which moved towards the NE, and at 12z 9/2/97 had reached a position just W of S Norway. In the original forecast the cyclone was under developed, the central pressure being about 8hPa higher than analysed at T+36. The position error was very slight, the cyclone being marginally too far eastwards at each stage of the forecast.

WV Image and PV Fields

At 0z 8/2/97 the WV image showed a strong dry feature associated with the trough in question. On the 315K & 300hPa surfaces a PV anomaly was located with its PV maximum (6 units) several degrees NE of the dry feature. The dry feature was located over the S flank of this PV anomaly. The anomaly was also apparent on upper troposhperic pressure surfaces.

PV Adjustments

It was (erroniously) considered that the relation between the dry feature and the PV anomaly represented a 'mismatch'. The PV adjustments therefore aimed to 'correct' this. The approach taken was to 'blank out' the PV anomaly and replace it with another PV anomaly constructed manually. The new anomaly was constructed to match the dry feature. This was done on pressure levels 250,300,350 & 400hPa.

Results

Four reruns were carried out, with different shapes and magnitudes for the reconstructed PV anomaly. Three of them had no significant impact on surface pressure development, but one of them did have a small positive impact. The central pressure of the cyclone deepened by about 3hPa at T+36, so reducing the intensity error from 8hPa to 5hPa. There was also a small change in the cyclone position, which did not reduce the position error, but neither did it increase it.

Despite the erronious assumption on which the PV adjustment was based in this case, a small positive impact on surface development was achieved.

CASE 3. 0Z 9/2/97 TO 0Z 10/2/97 IOP12

Original Forecast

This case focused on the development of a large N Atlantic cyclone, located between Greenland and Iceland; the cyclone was somewhat under developed by the forecast. There was very little position error, but the cyclone did not move much over the 24 hour forecast period anyway.

WV Image and PV Fields

The relation between the wv image and the 315K PV field was complex and difficult to understand in this case. Three prominent dry features appear in the wv image, with associated anomalies or sharp gradients in the 315K PV field. One respect in which the PV field appears to be mismatched with the image is that there is a moist or cloudy region, encompassed by the three dry features, which has a complex pattern of PV contours crossing it. It is believed that such regions should be relatively free of PV contours, and that the contours should in fact follow the edge of the moist or cloudy region.

PV Adjustments & Results

The same approach was used as in case 1, i.e., the satellite WV image was scaled to PV units and a cut-out portion of it was used as substitute PV, and pasted into the UM initial PV field. This adjustment was carried out in the vicinity of the most southerly one of the three dry features, in the belief that this would have the most impact on the surface development. This procedure was followed on pressure levels 300,350,400,450 & 500hPa, with appropriate scaling factors for each level. There was a small negative impact on surface pressure development.

CASE 4. 12Z 1/9/97 TO 12Z 3/9/97

Original Forecast

In the anlysis a mid-Atlantic cyclone (due S of Greenland) appeared at an early stage of development at 12z 1/9/97 (fig. 5.4.1). It moved eastwards and deepened, reaching a location off the W coast of Scotland at 12z 3/9/97 (fig. 5.4.2). In the original forecast the cyclone was under developed at each stage of the forecast by 3-4hPa. There was a slight position error, the forecast track being marginally south of the correct track (fig. 5.4.3).

WV Image and PV Fields

The WV image at 12z 1/9/97 (fig. 5.4.4) shows a small dry feature associated with the developing cyclone, and the 250 & 300hPa PV fields show a PV anomaly clearly associated with the dry feature. This anomaly does not extend much below 300hPa; it is not apparent at 350hPa. The peak of the anomaly (magnitude about 4 units) lies a little to the N of the dry feature, which curves around the S flank of the anomaly.

PV Adjustments

The relation between the dry feature and the PV anomaly appears to be correct as far as spatial location and orientation is concerned. At the time that this case study was carried out, it was thought (erroniously) that the PV maximum should coincide with the dry feature, and the position of the PV anomaly was adjusted accordingly. This small adjustment in position probably had little if any influence on surface development. However, what is more significant is that the PV anomaly was extended vertically to lower levels, and its magnitude was enhanced (fig.5.4.5). This did have a significant effect on surface devevlopment.

Results

Three reruns were performed, with increasing degrees of enhancement and vertical extension to the PV anomaly. In rerun 3 the anomaly was extended down to 500hPa and its magnitude enhanced by a factor of 1.6 at 250hPa, and by smaller factors on other levels. (These adjustments were arrived at purely by trial and error). In rerun 3 the error in forecast depth of the cyclone was greatly reduced; at T+36 there was virtually no error (fig. 5.4.6). There was also a slight improvement in forecast track of the low centre, which moved slightly N, although it was now slightly too far W.

This result indicates that it is relatively easy to correct depth errors in compact cyclones by changing the magnitude and/or vertical extent of the associated PV anomaly. It also seems to indicate that correction of position errors is rather more difficult.

CASE 5. 12Z 8/9/97 TO 12Z 10/9/97

The synoptic situation for this case was dominated by a large anticyclonic system which covered much of the N Atlantic. The only cyclonic development which occurred was well to the N of the PV inversion domain and so provided no scope at all for PV adjustment.

Fig. 5.4.1 Case 4 PMSL analysis 12z 1/9/97

Fig. 5.4.2 Case 4 PMSL analyses, 12hr intervals from 0z 2/9/97

Fig. 5.4.3 Case 4 PMSL original forecast T+12 to T+48

Fig. 5.4.4 Case 4 Background WV image 12z 1/9/97
Contours PV at 300hPa, from analysis
Range 0-12 PVU, Interval 1 PVU

Fig. 5.4.5 Case 4 Rerun 3 Background WV image 12z 1/9/97
Contours PV on 300hPa
Range 0-12 PVU, interval 1 PVU

Fig. 5.4.6 Case 4 Rerun 3 PMSL T+12 to T+48

XAATG Mean sea Level Atmos pressure at mean sea level
At 12Z on 1/ 9/1997, from 12Z on 1/ 9/1997

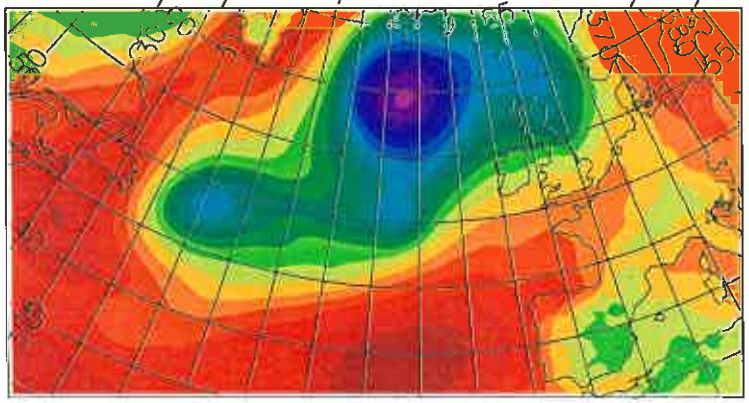

99400 99800 100200 100600 101000 101400 101800 102200 102600

XAATG Mean sea Level Atmos pressure at mean sea level
At 00Z on 2/ 9/1997, from 00Z on 2/ 9/1997

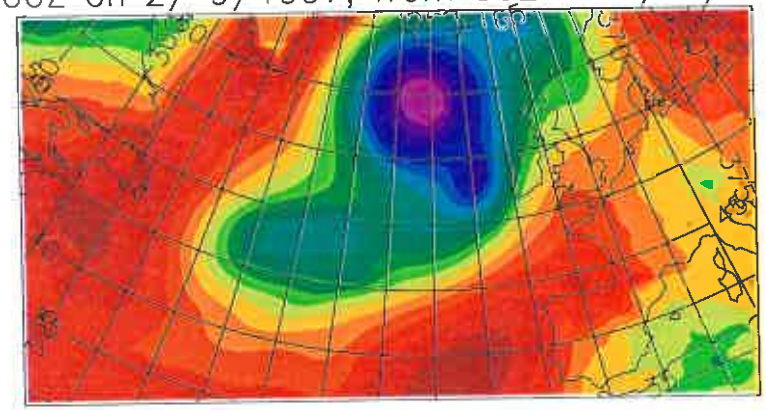

XAATG Mean sea Level Atmos pressure at mean sea level
At 12Z on 2/ 9/1997, from 12Z on 2/ 9/1997

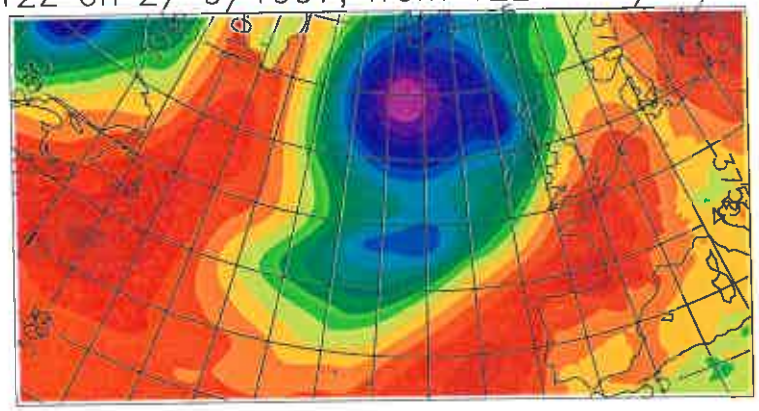

XAATG Mean sea Level Atmos pressure at mean sea level
At 00Z on 3/ 9/1997, from 00Z on 3/ 9/1997

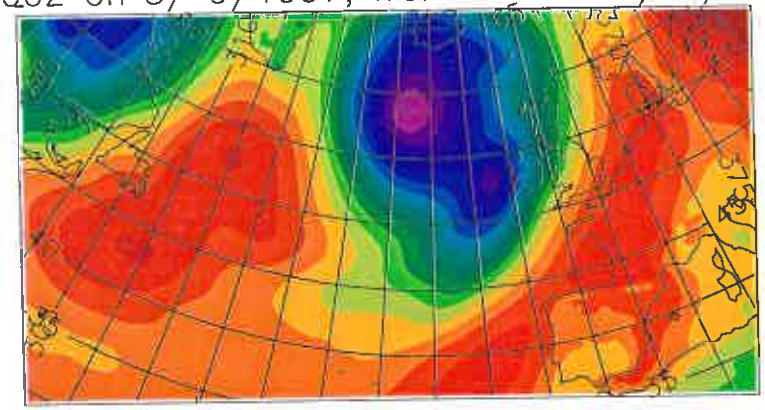

XAATG Mean sea Level Atmos pressure at mean sea level
At 12Z on 3/ 9/1997, from 12Z on 3/ 9/1997

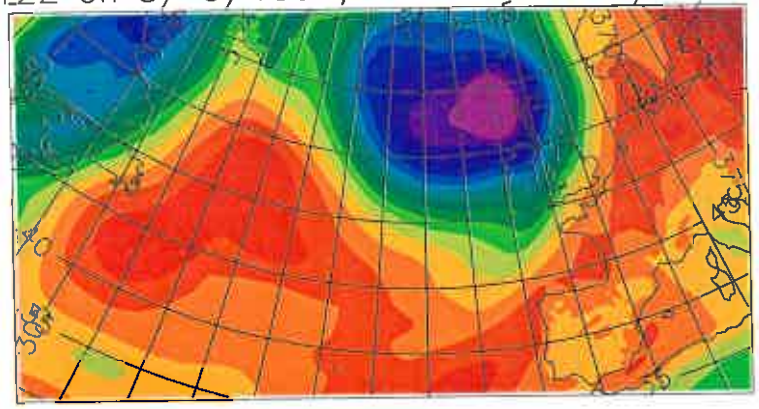

XAATH Mean sea Level Atmos pressure at mean sea level
At 00Z on 2/ 9/1997, from 12Z on 1/ 9/1997

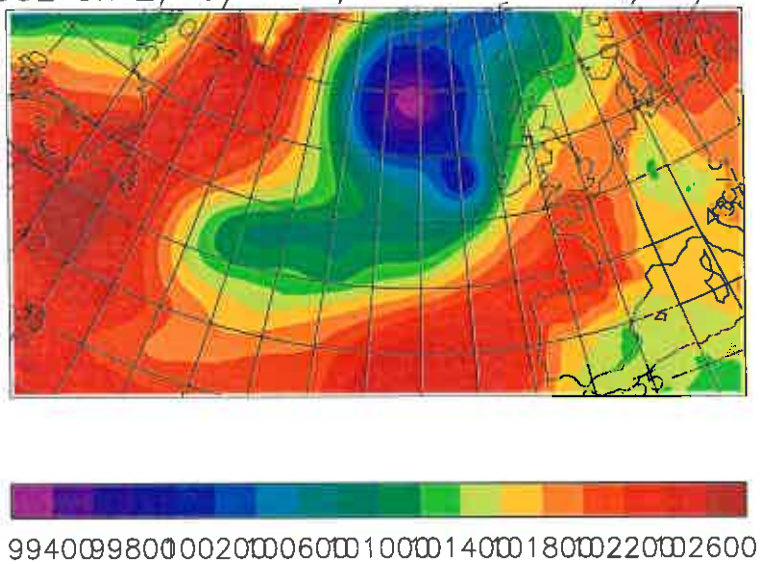

9940099800100200060001000014000180002200026000

XAATH Mean sea Level Atmos pressure at mean sea level
At 12Z on 2/ 9/1997, from 12Z on 1/ 9/1997

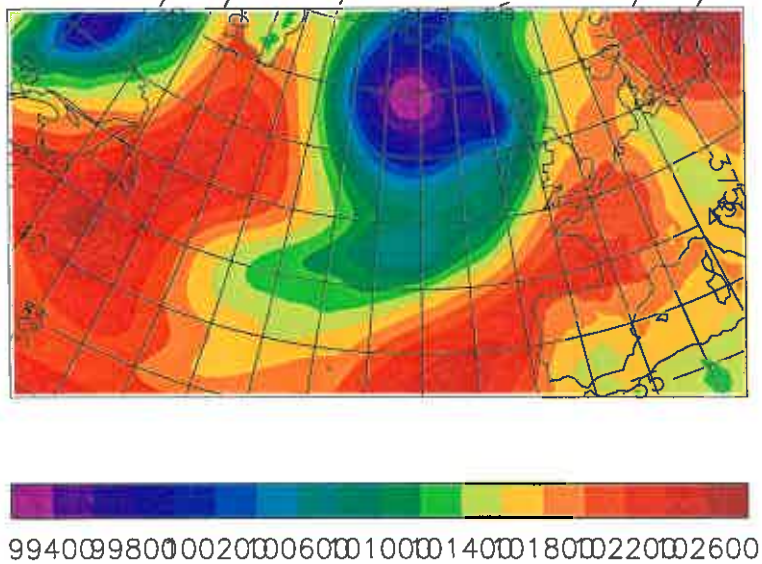

9940099800100200060001000014000180002200026000

XAATH Mean sea Level Atmos pressure at mean sea level
At 00Z on 3/ 9/1997, from 12Z on 1/ 9/1997

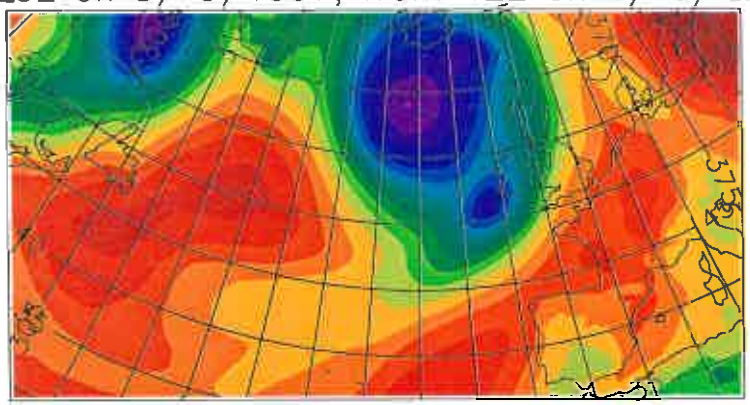

9940099800100200060001000014000180002200026000

XAATH Mean sea Level Atmos pressure at mean sea level
At 12Z on 3/ 9/1997, from 12Z on 1/ 9/1997

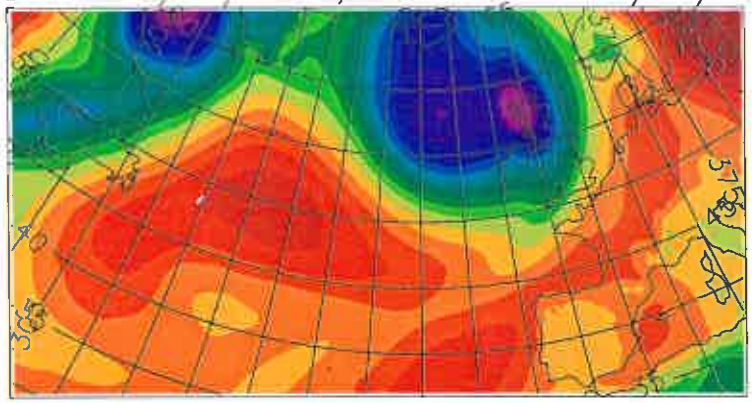

9940099800100200060001000014000180002200026000

XAACP surface Atmos wv satellite image
At 12Z on 1/ 9/1997, from 12Z on 1/ 9/1997

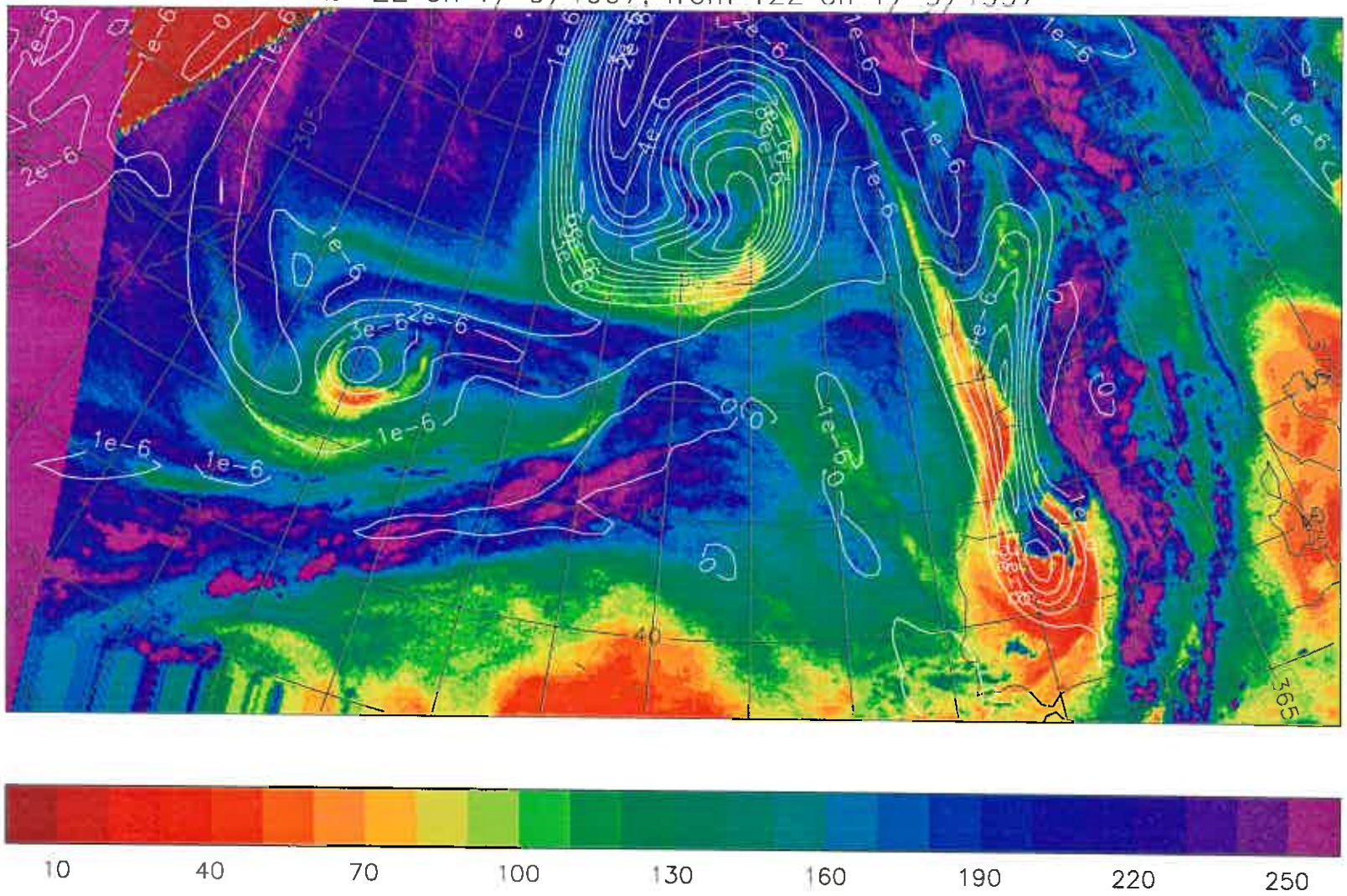

XAACP surface Atmos wv satellite image
At 12Z on 1/ 9/1997, from 12Z on 1/ 9/1997

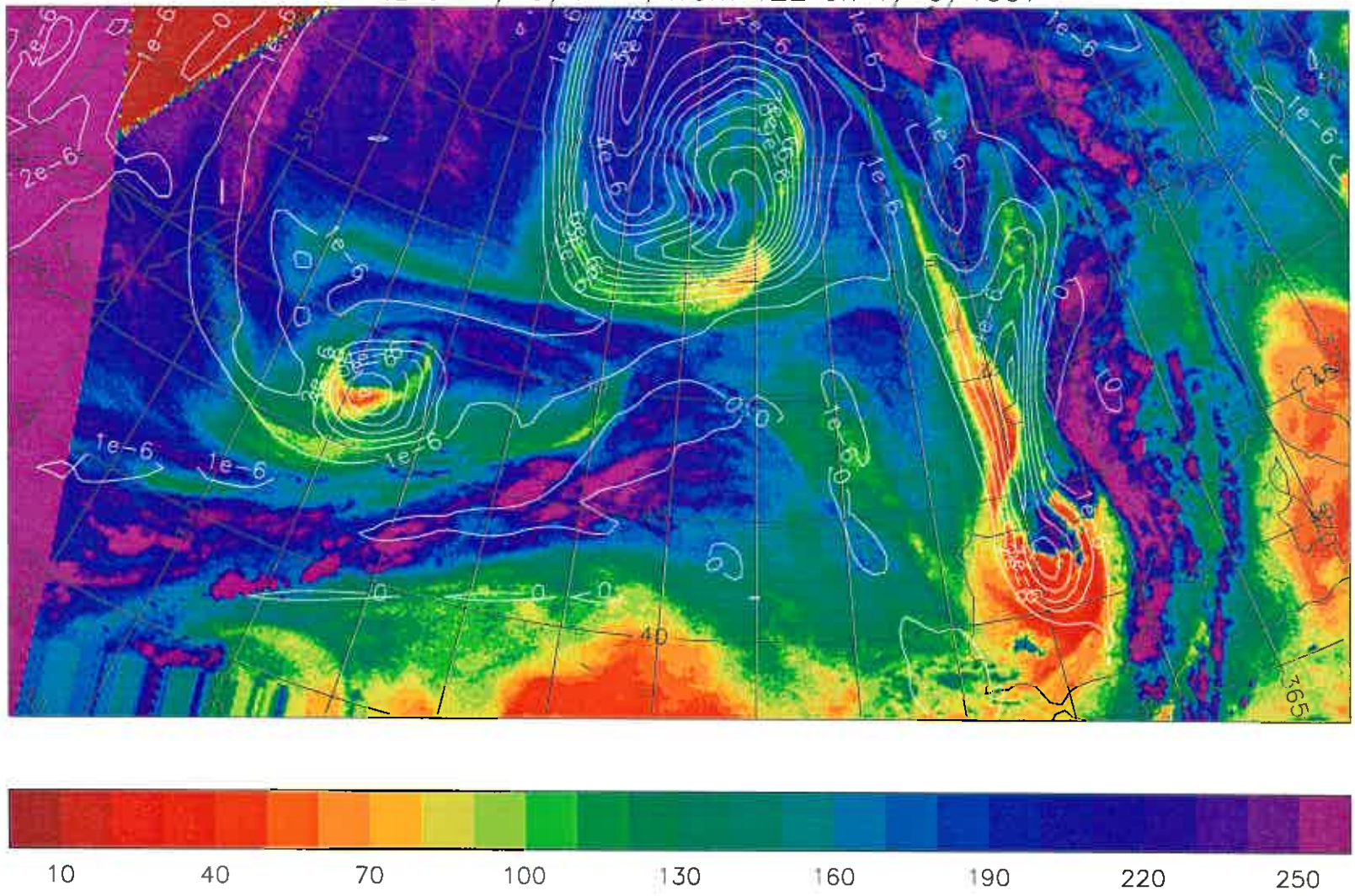

XAATH Mean sea Level Atmos pressure at mean sea level
At 00Z on 2/ 9/1997, from 12Z on 1/ 9/1997

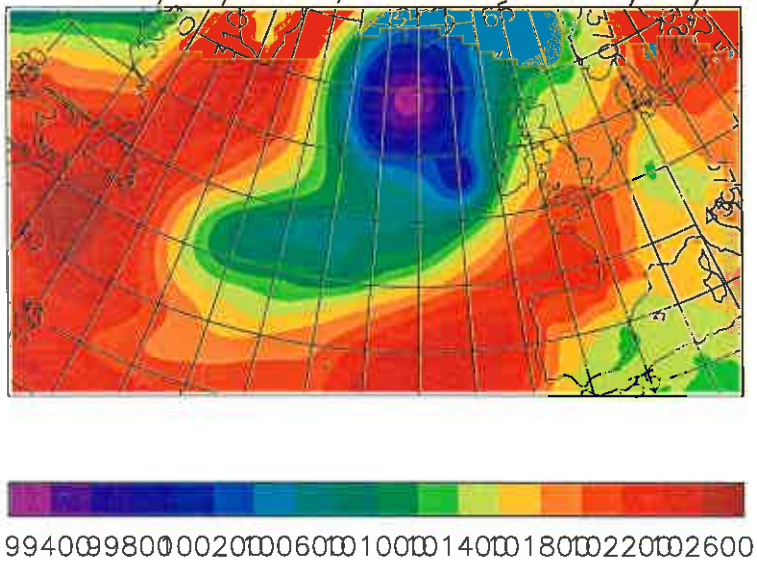

9940 9980 10020 10060 10100 10140 10180 10220 10260

XAATH Mean sea Level Atmos pressure at mean sea level
At 12Z on 2/ 9/1997, from 12Z on 1/ 9/1997

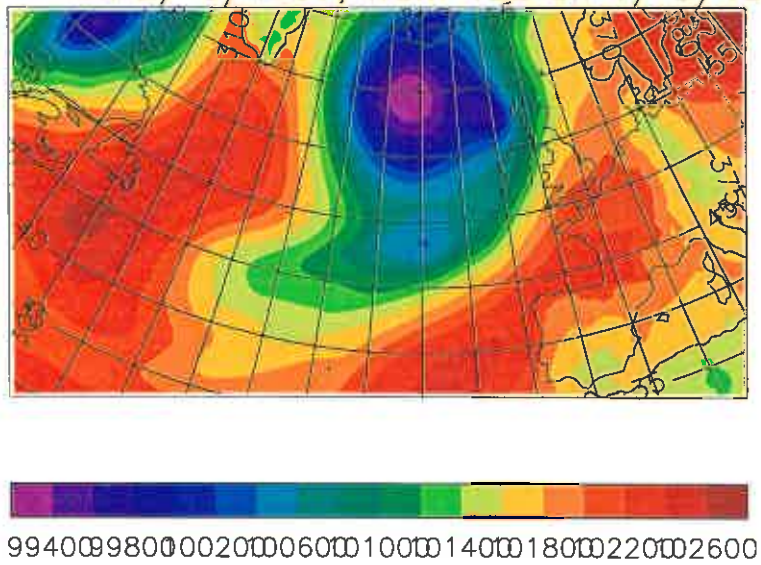

9940 9980 10020 10060 10100 10140 10180 10220 10260

XAATH Mean sea Level Atmos pressure at mean sea level
At 00Z on 3/ 9/1997, from 12Z on 1/ 9/1997

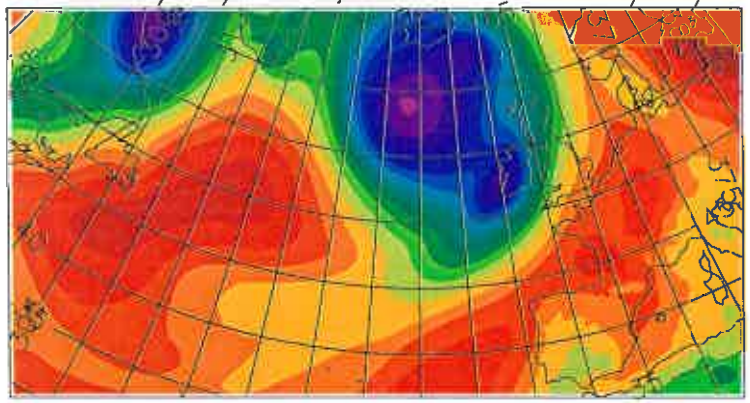

9940 9980 10020 10060 10100 10140 10180 10220 10260

XAATH Mean sea Level Atmos pressure at mean sea level
At 12Z on 3/ 9/1997, from 12Z on 1/ 9/1997

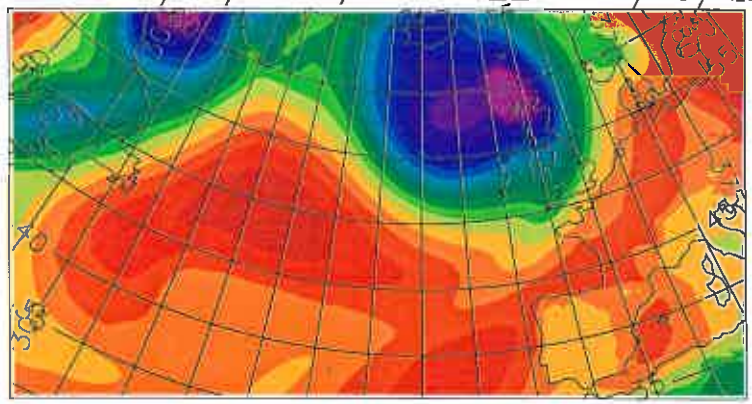

9940 9980 10020 10060 10100 10140 10180 10220 10260

CASE 6. 12Z 15/9/97 TO 12Z 17/9/97

Original Forecast

At 12z 15/9/97 the analysis showed a large developed cyclone just S of Iceland (fig. 5.6.1). This system moved towards Scandinavia and decayed over the forecast period (fig. 5.6.2). By T+36 it lay just W of S Sweden. In the original forecast this system decayed rather too quickly, its central pressure being about 4hPa too high at T+24 and T+36 (fig. 5.6.3). Its position was essentially correct throughout.

It is of interest also to note an intense circular depression in mid-Atlantic at the latitude of N Spain, which moves NW and fills somewhat over the forecast period. This is presumably a tropical storm which has moved over from the Carribean. In the forecast this system also filled a little too quickly and also tracked a few degrees too far N.

WV Image and PV Fields

The WV image at 12z 15/9/97 (fig. 5.6.4) shows a prominent dry feature corresponding to the Icelandic cyclone. It curves around the S flank of a PV anomaly which is clearly visible on the 330K and 300hPa surfaces (figs. 5.6.4, 5.6.5). This anomaly extends vertically downwards, and is still clearly visible at 500hPa.

The PV anomaly corresponding to the tropical depression was essentially a lower level feature; it was just visible at 350hPa, and became more prominent at 400 & 500hPa. It would very probably have extended down to the earth's surface.

PV Adjustments

The PV adjustments were related to the Icelandic depression only; no attempt was made to adjust the PV associated with the tropical system. This case presented a serious practical difficulty, in that the PV anomaly of interest lay partly beyond the PV inversion domain N boundary. This boundary is imposed by the need to avoid encroachment on Greenland, if the vertical extent of the PV inversion domain is to extend below 600hPa. The results of the PV adjustment and inversion were therefore rather unsatisfactory in that only the part of the PV anomaly lying S of the tip of Greenland could be adjusted, and a large 'domain edge oscillation' was generated by the inversion process.

Despite these difficulties, two reruns were carried out. In rerun 1 (fig. 5.6.6) the PV anomaly was moved a few degrees S, closer to the dry WV feature, and also scaled up by a factor of 1.3. This was done on levels 250,300,350,400,450 & 500 hPa. In rerun 2 the scaling was carried out, but the PV anomaly was not moved.

Results

Rerun 1 (fig. 5.6.7) shows a positive impact on surface development, in that the cyclone is deepened to virtually the correct extent at each stage of the forecast. The effect on the shape and position of the cyclone was slightly detrimental. Rerun 2 also shows a positive impact, but not as much as in rerun 1.

Fig. 5.6.1 Case 6 PMSL analysis 12z 15/9/97 (upper left frame)

Fig. 5.6.2 Case 6 PMSL analyses, 12hr intervals from 0z 15/9/97

Fig. 5.6.3 Case 6 PMSL original forecast T+12 to T+48

Fig. 5.6.4 Case 6 Background WV image 12z 15/9/97
Contours PV at 300hPa, from analysis
Range 0-12 PVU, Interval 1 PVU

Fig. 5.6.5 Case 6 PV on 250 & 300hPa 12z 15/9/97
Range 0-12 PVU

Fig. 5.6.6 Case 6 Rerun 1 PV on 250 & 300hPa T+0
Range -4 -12 PVU

Fig. 5.6.7 Case 6 Rerun 1 PMSL T+12 to T+48

XAATG Mean sea Level Atmos pressure at mean sea level
At 12Z on 15/ 9/1997, from 12Z on 15/ 9/1997

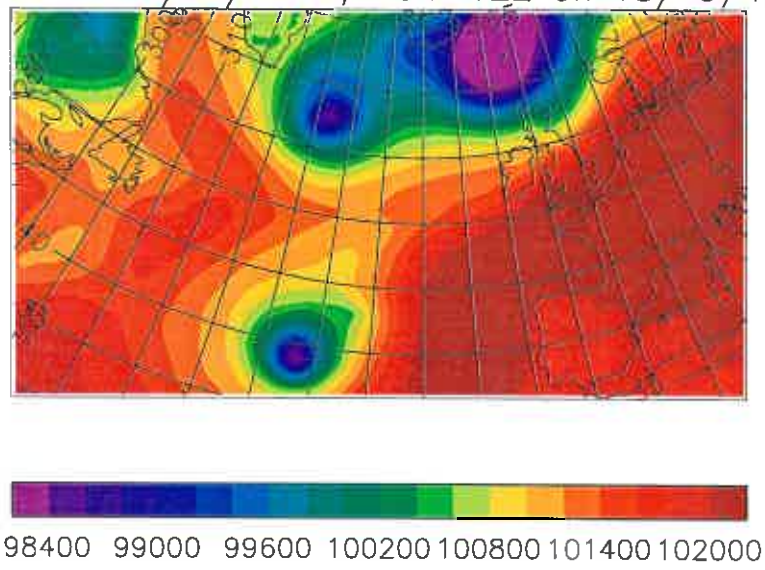

98400 99000 99600 100200 100800 101400 102000

XAATG Mean sea Level Atmos pressure at mean sea level
At 12Z on 16/ 9/1997, from 12Z on 16/ 9/1997

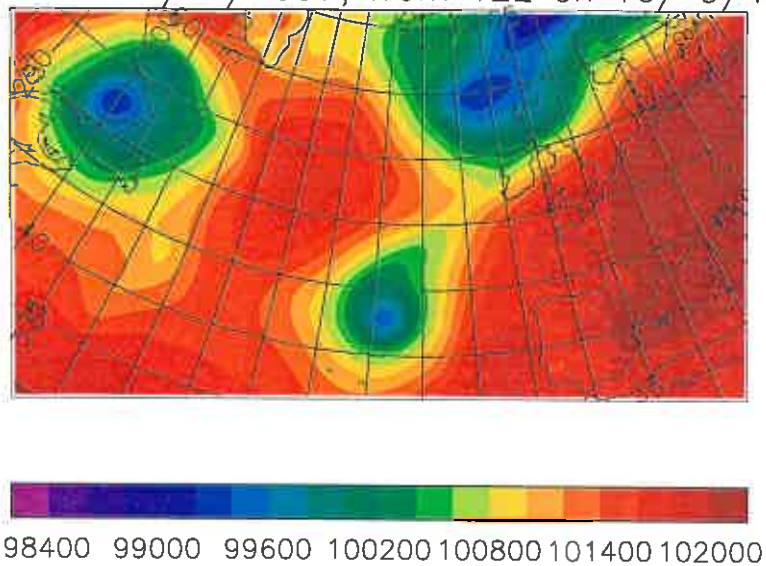

98400 99000 99600 100200 100800 101400 102000

XAATG Mean sea Level Atmos pressure at mean sea level
At 00Z on 17/ 9/1997, from 00Z on 17/ 9/1997

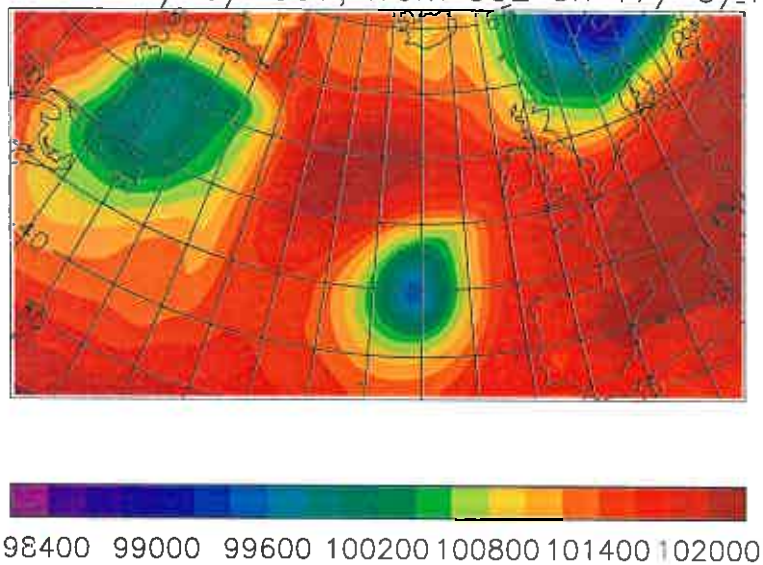

98400 99000 99600 100200 100800 101400 102000

XAATG Mean sea Level Atmos pressure at mean sea level
At 12Z on 17/ 9/1997, from 12Z on 17/ 9/1997

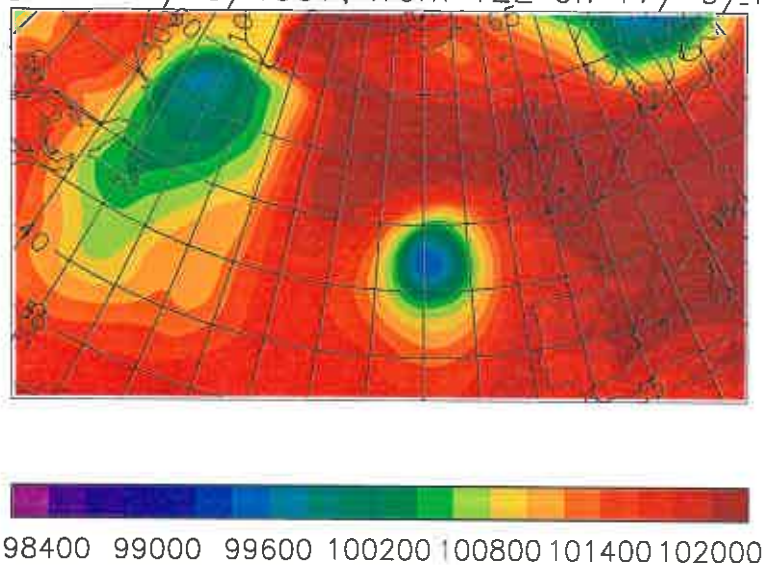

98400 99000 99600 100200 100800 101400 102000

XAATH Mean sea Level Atmos pressure at mean sea level
At 00Z on 16/ 9/1997, from 12Z on 15/ 9/1997

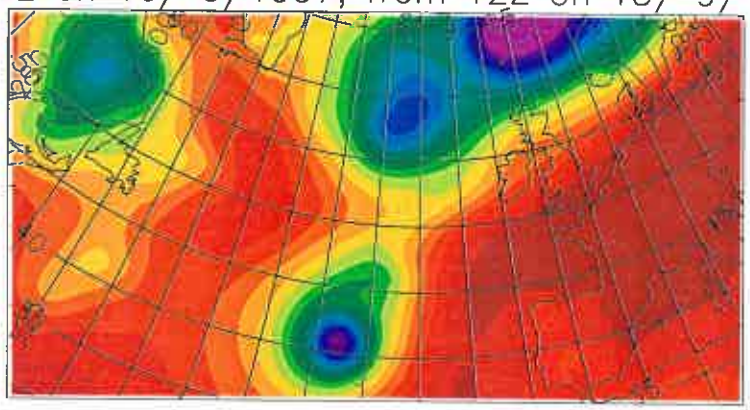

98400 99000 99600 100200 100800 101400 102000

XAATH Mean sea Level Atmos pressure at mean sea level
At 12Z on 16/ 9/1997, from 12Z on 15/ 9/1997

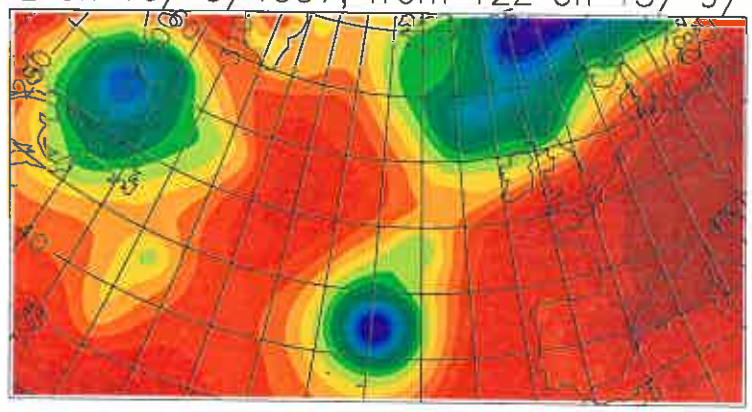

98400 99000 99600 100200 100800 101400 102000

XAATH Mean sea Level Atmos pressure at mean sea level
At 00Z on 17/ 9/1997, from 12Z on 15/ 9/1997

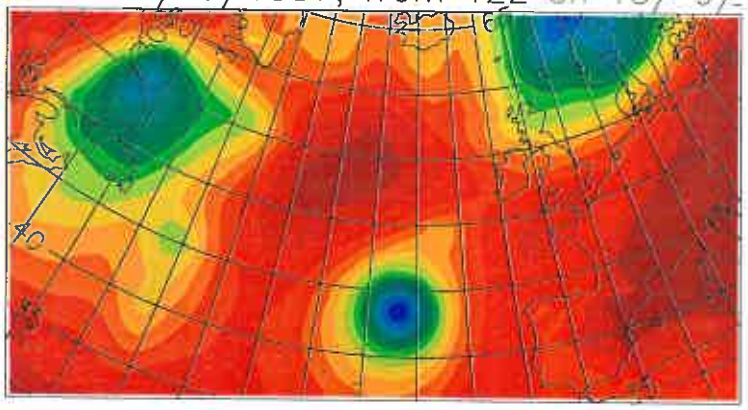

98400 99000 99600 100200 100800 101400 102000

XAATH Mean sea Level Atmos pressure at mean sea level
At 12Z on 17/ 9/1997, from 12Z on 15/ 9/1997

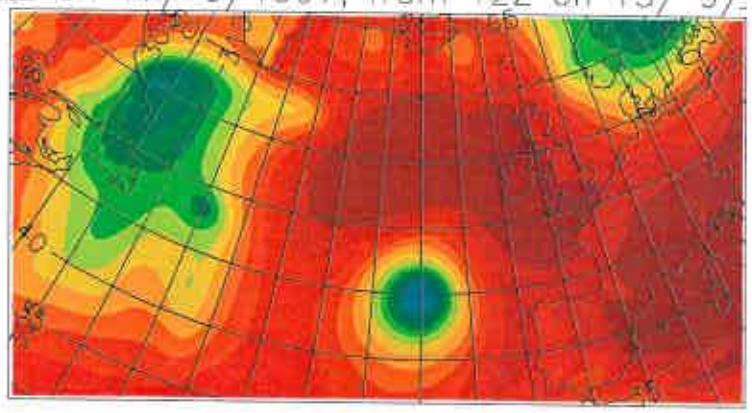

98400 99000 99600 100200 100800 101400 102000

XAACP surface Atmos wv satellite image
At 12Z on 15/ 9/1997, from 12Z on 15/ 9/1997

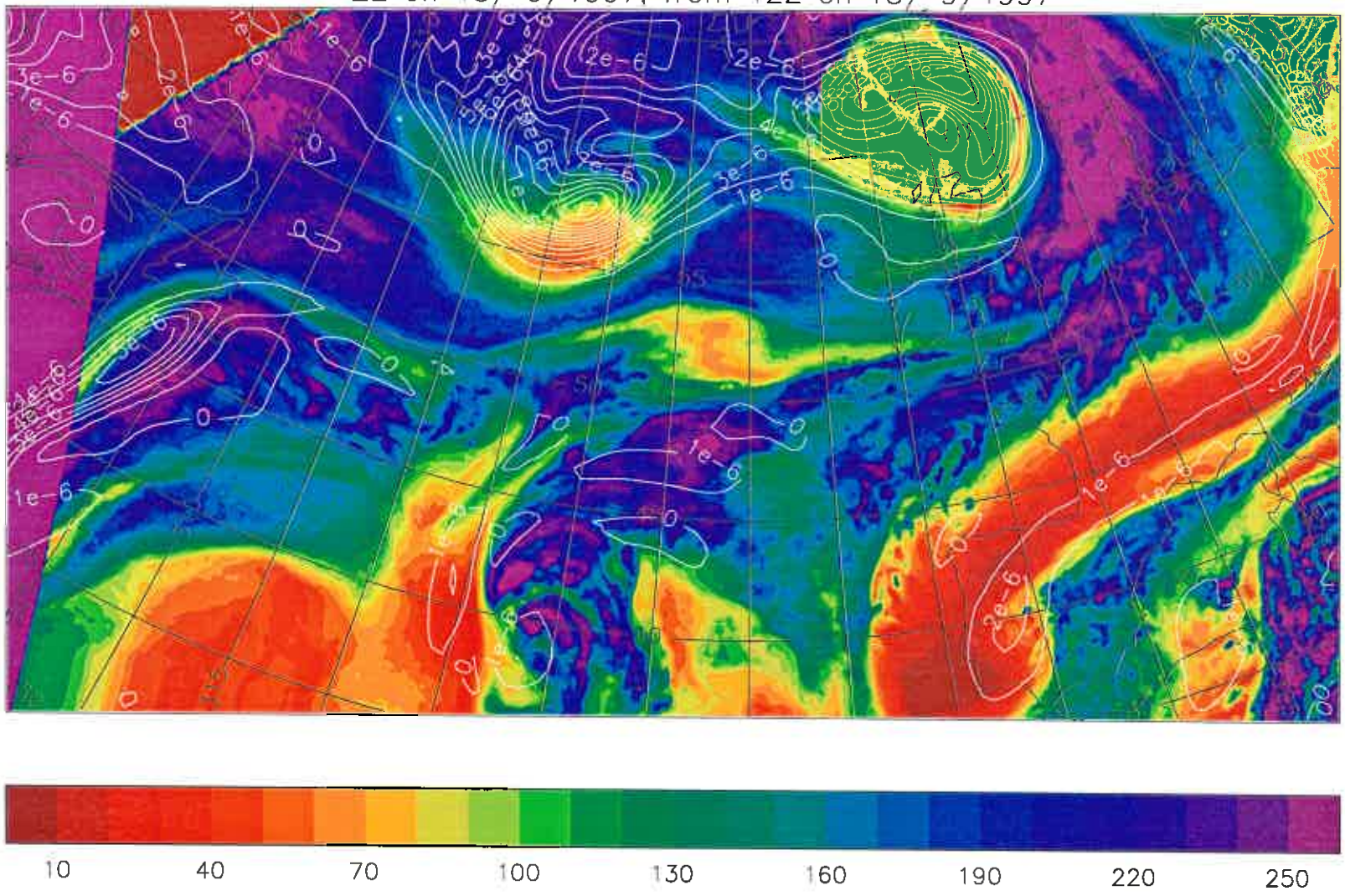

XAATG Atmos potential vorticity on pressure levs at 250.0 hPa
At 12Z on 15/ 9/1997, from 12Z on 15/ 9/1997

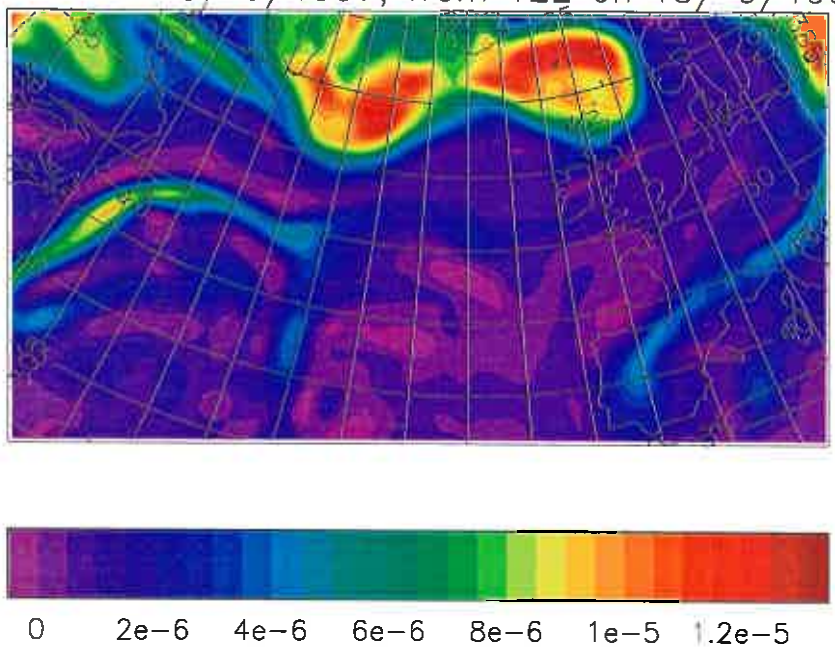

XAATG Atmos potential vorticity on pressure levs at 300.0 hPa
At 12Z on 15/ 9/1997, from 12Z on 15/ 9/1997

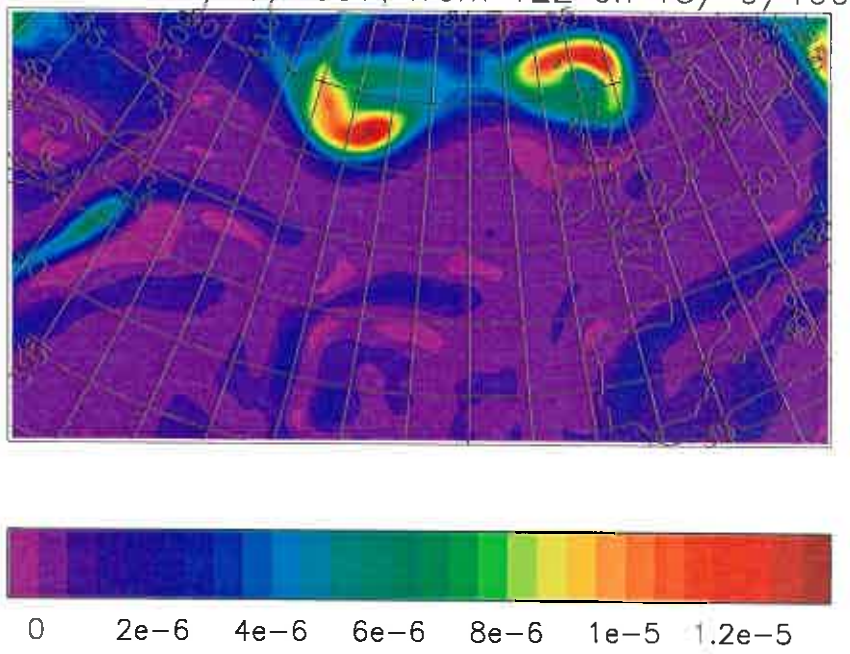

XAATH Atmos potential vorticity on pressure levs at 250.0 hPa
At 12Z on 15/ 9/1997, from 12Z on 15/ 9/1997

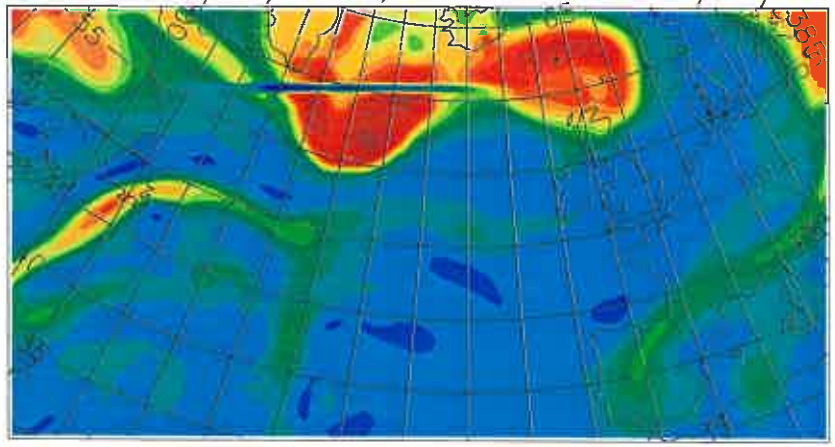

XAATH Atmos potential vorticity on pressure levs at 300.0 hPa
At 12Z on 15/ 9/1997, from 12Z on 15/ 9/1997

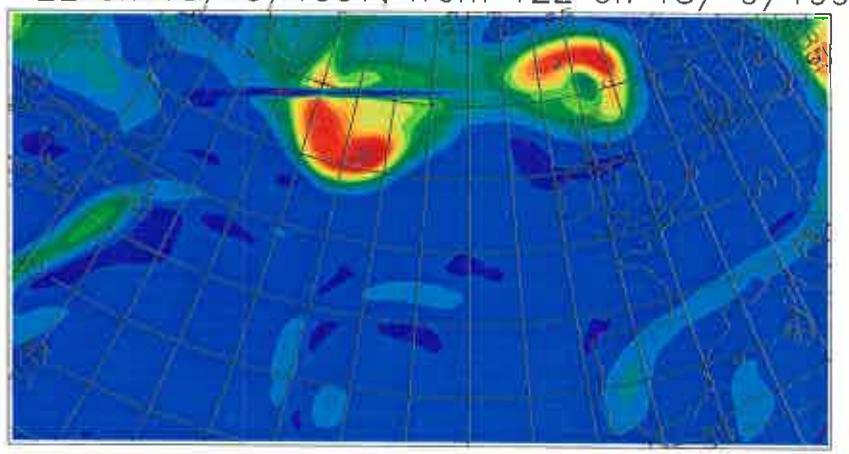

XAATH Mean sea Level Atmos pressure at mean sea level
At 00Z on 16/ 9/1997, from 12Z on 15/ 9/1997

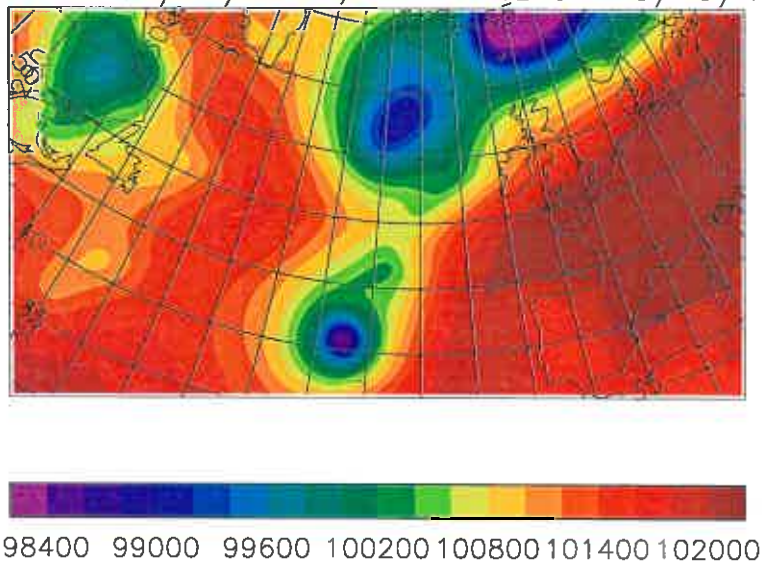

98400 99000 99600 100200 100800 101400 102000

XAATH Mean sea Level Atmos pressure at mean sea level
At 12Z on 16/ 9/1997, from 12Z on 15/ 9/1997

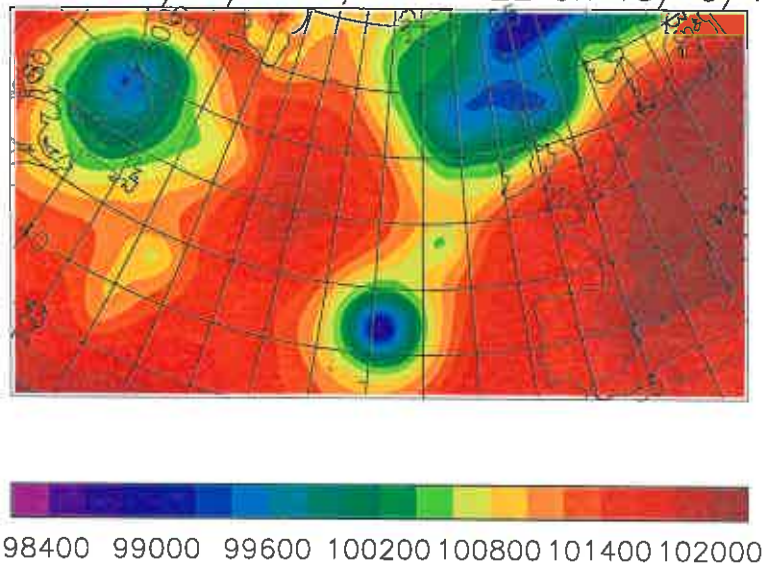

98400 99000 99600 100200 100800 101400 102000

XAATH Mean sea Level Atmos pressure at mean sea level
At 00Z on 17/ 9/1997, from 12Z on 15/ 9/1997

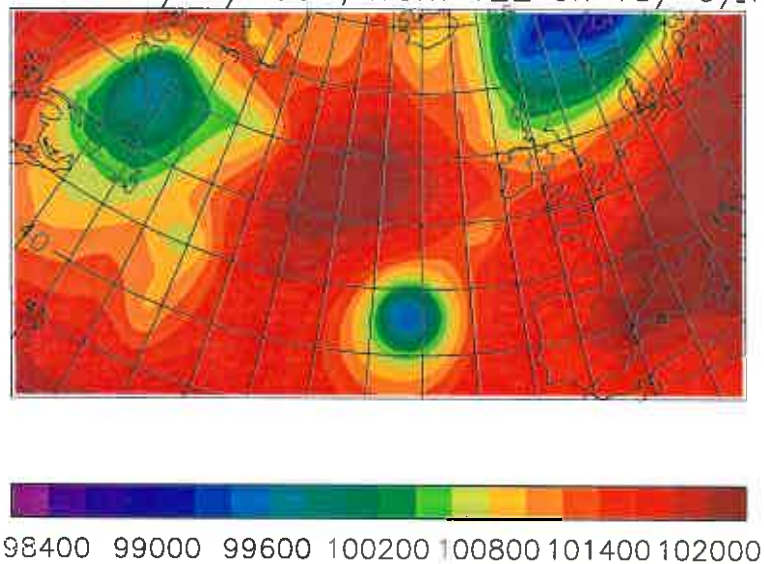

98400 99000 99600 100200 100800 101400 102000

XAATH Mean sea Level Atmos pressure at mean sea level
At 12Z on 17/ 9/1997, from 12Z on 15/ 9/1997

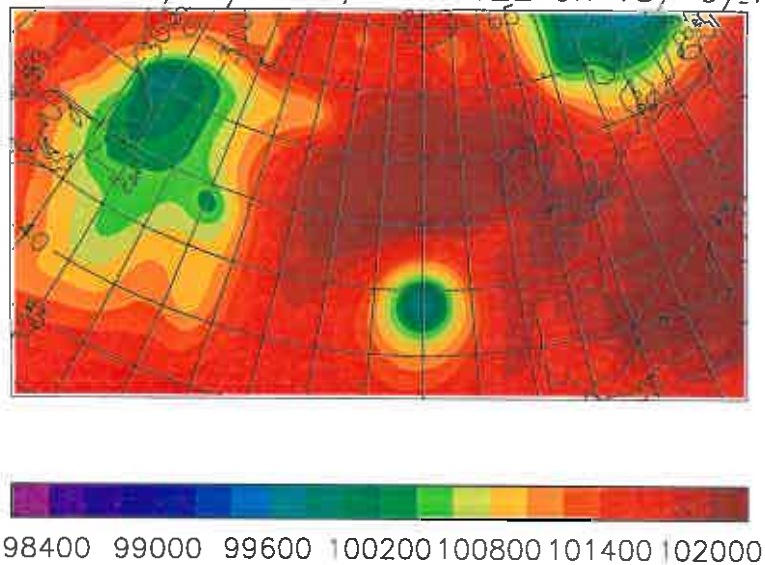

98400 99000 99600 100200 100800 101400 102000

CASE 7. 12Z 22/9/97 TO 12Z 24/9/97

Original Forecast

At 12z 22/9/97 the analysis has decaying cyclone to the SW of the British Isles. It continued to decay over the subsequent 48 hours without changing its position. In the original forecast this system decayed too rapidly.

The 12z 23/9/97 analysis showed another cyclone beginning to devlop over E Canada; by 12z 24/9/97 it had developed into a large system centred over the NW Atlantic just off E Canada, its central pressure having deepened by 12-14hPa. In the original forecast this system was in the correct location but was under developed.

Over the same period a large anticyclonic area developed in mid-Atlantic. This was under developed in the orginal forecast.

WV Image and PV Fields

The 300hPa PV field at showed a large intense anomaly, roughly circular in form and co-located with the decaying cyclone SW of the British Isles. This anomaly was not apparent on 350hPa or any lower level. Associated with this, the WV image showed a large intense dry intrusion feature running N-S down the W flank of the PV anomaly. This feature had its own PV signature in the 300hPa field, co-located with the dry intrusion and of a similar shape and orientation. This PV structure was visible as a discrete feature down to 350hPa, but from 400hPa it began to merge with adjacent PV structures and so became less distinct.

This relationship, between a roughly circular PV anomaly and an associated dry intrusion feature, is of a type which is virtually always seen in cyclonic development. The PV anomaly represents a local depression in the tropopause, and the dry intrusion feature in the WV image represents, in general, a stream of stratospheric and upper-tropospheric air which is drawn around the tropopause depression. Typically, the 300hPa level intersects the tropopause depression, and so the tropopause depression is the most intense PV feature at such levels. Its PV maximum acts like a 'pivot point' for the dry intrusion. The dry intrusion itself also has relatively high PV, but its PV signature is less prominent than the tropopause depression signature at this level. At levels a little below the tropopause depression (typically 400-500hPa), the tropopause depression is no longer visible as a PV structure, so the PV signature of the dry intrusion is the most prominent feature.

The WV image also showed another elongated dry feature off E Canada, associated with the cyclonic development in that vicinity. The 300hPa PV field showed a large complex are of high PV over E Canada. This area was bounded by a region of sharp PV gradient matching precisely in position and form with the elongated dry feature.

PV Adjustments and Rerun Results

Three reruns were performed. We consider only the effect on MSLP.

Rerun 1 : In this rerun the circular PV anomaly associated with the tropopause depression was enhanced on 300hPa (by a factor of 1.2); on the 350, 400 & 450hPa levels a scaled-down copy of this anomaly was introduced. This markedly deepened the decaying cyclone SW of the British Isles up to T+24, so that it actually became a

XAATH Mean sea Level Atmos pressure at mean sea level
At 06Z on 13/10/1997, from 06Z on 13/10/1997

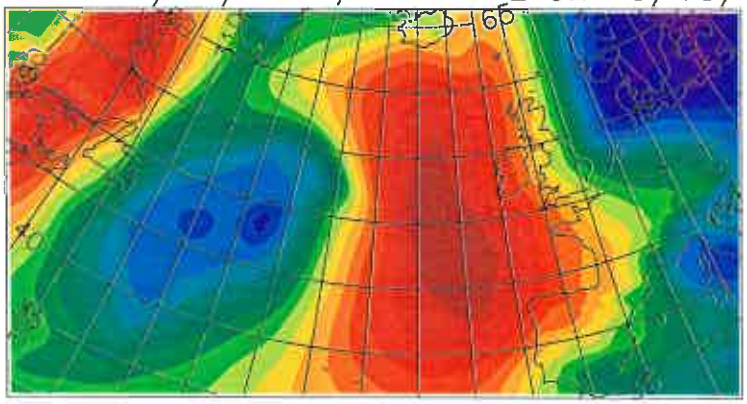

99400 100000 100600 101200 101800 102400 103000

XAATC Atmos potential vorticity on pressure levs at 250.0 hPa
At 06Z on 13/10/1997, from 06Z on 13/10/1997

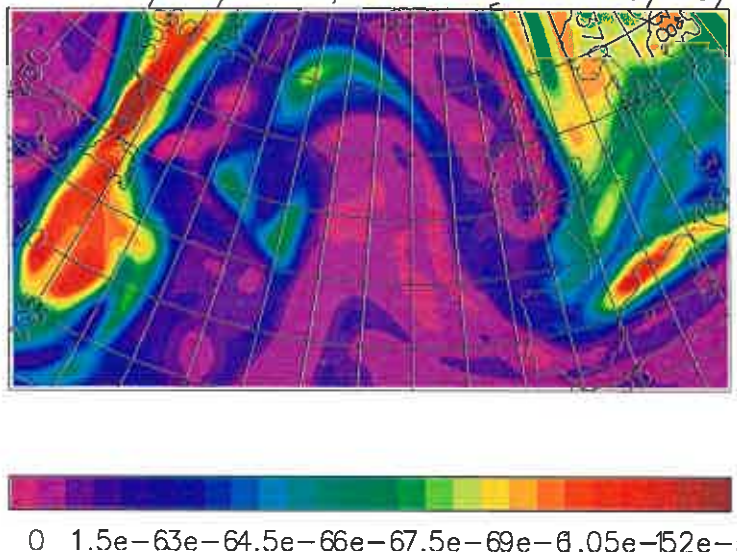

0 1.5e−63e−64.5e−66e−67.5e−69e−6 1.05e−52e−5

XAATJ Atmos potential vorticity on pressure levs at 250.0 hPa
At 06Z on 13/10/1997, from 06Z on 13/10/1997

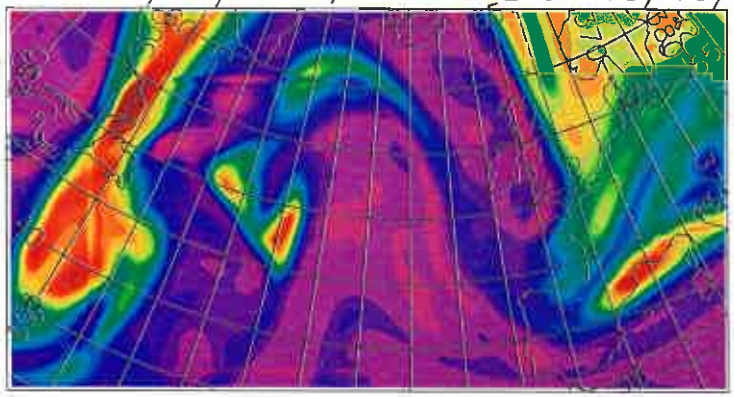

0 1.5e−63e−64.5e−66e−67.5e−69e−6 1.05e−52e−5

XAATD Mean sea Level Atmos pressure at mean sea
At 12Z on 13/10/1997, from 12Z on 13/10/19

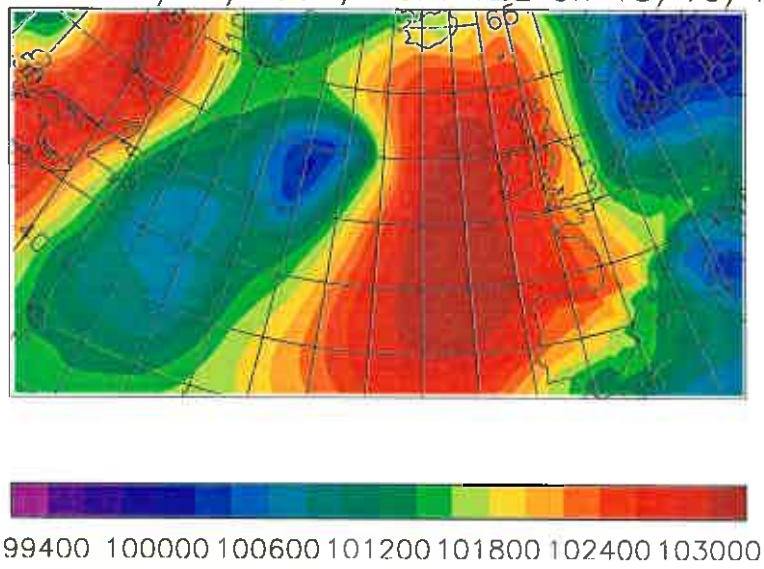

99400 100000 100600 101200 101800 102400 103000

XAATE Mean sea Level Atmos pressure at mean sea level
At 18Z on 13/10/1997, from 18Z on 13/10/1997

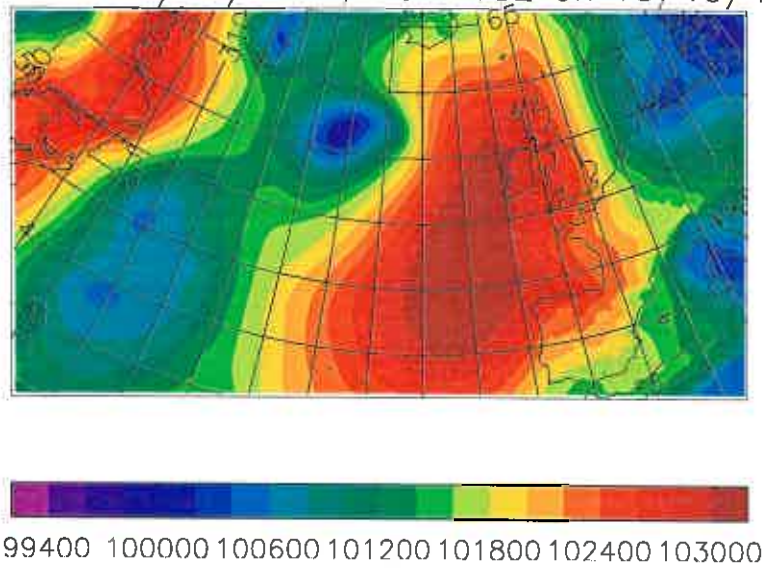

99400 100000 100600 101200 101800 102400 103000

XAATF Mean sea Level Atmos pressure at mean sea
At 00Z on 14/10/1997, from 00Z on 14/10/19

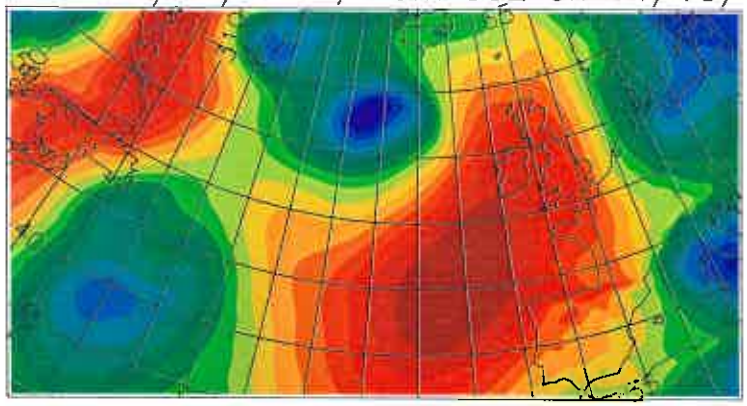

99400 100000 100600 101200 101800 102400 103000

XAATG Mean sea Level Atmos pressure at mean sea level
At 06Z on 14/10/1997, from 06Z on 14/10/1997

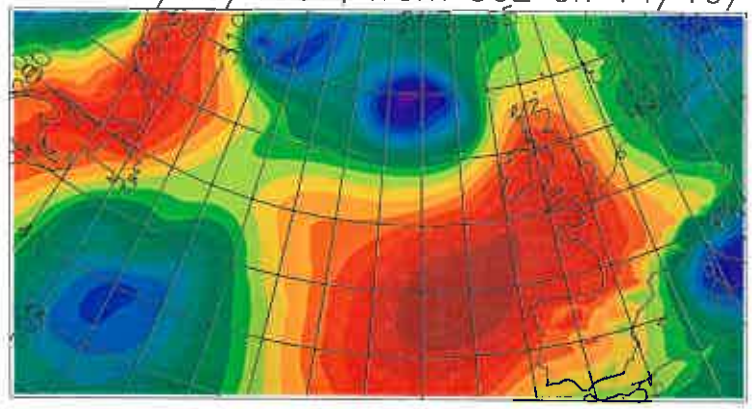

99400 100000 100600 101200 101800 102400 103000

XAATH Mean sea Level Atmos pressure at mean sea
At 12Z on 13/10/1997, from 06Z on 13/10/19

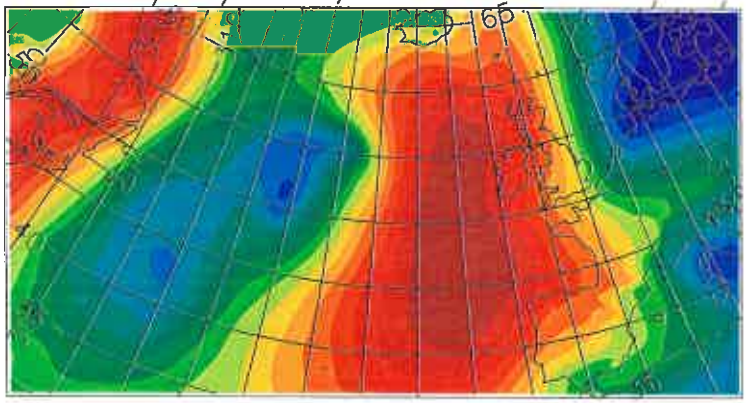

99400 100000 100600 101200 101800 102400 103000

XAATH Mean sea Level Atmos pressure at mean sea level
At 18Z on 13/10/1997, from 06Z on 13/10/1997

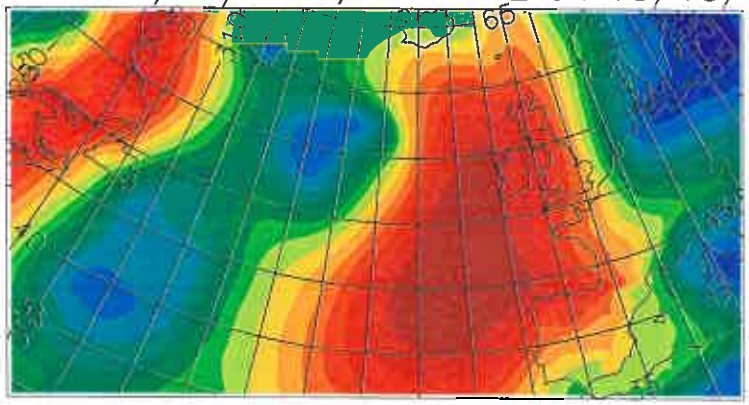

99400 100000 100600 101200 101800 102400 103000

XAATH Mean sea Level Atmos pressure at mean sea
At 00Z on 14/10/1997, from 06Z on 13/10/19

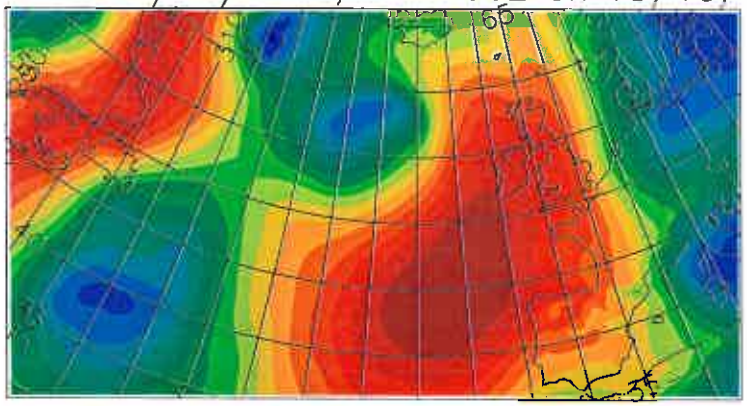

99400 100000 100600 101200 101800 102400 103000

XAATH Mean sea Level Atmos pressure at mean sea level
At 06Z on 14/10/1997, from 06Z on 13/10/1997

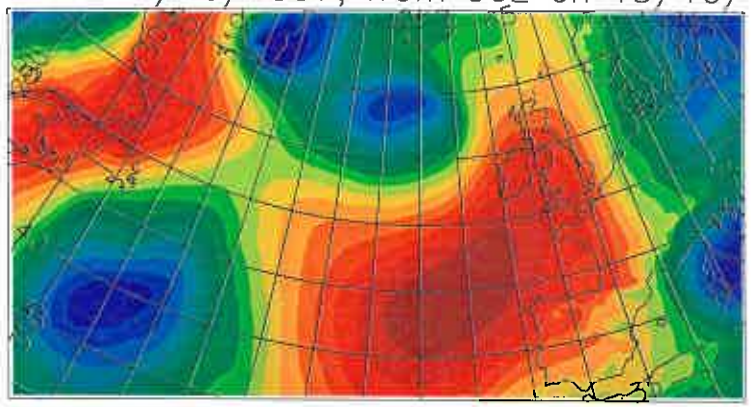

99400 100000 100600 101200 101800 102400 103000

XAACP surface Atmos wv satellite image
At 06Z on 13/10/1997, from 06Z on 13/10/1997

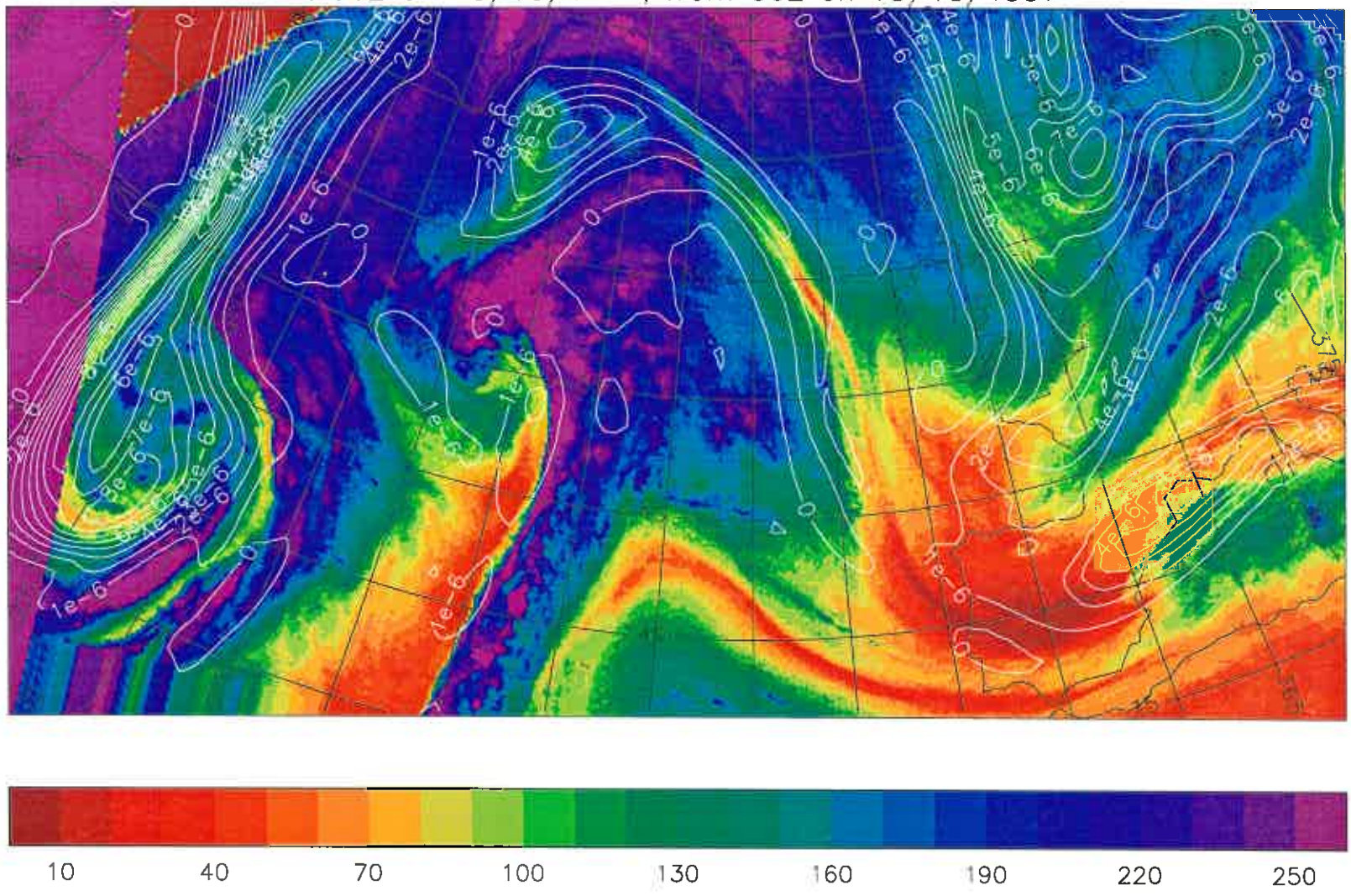

XAATH Mean sea Level Atmos pressure at mean sea
At 12Z on 13/10/1997, from 06Z on 13/10/19

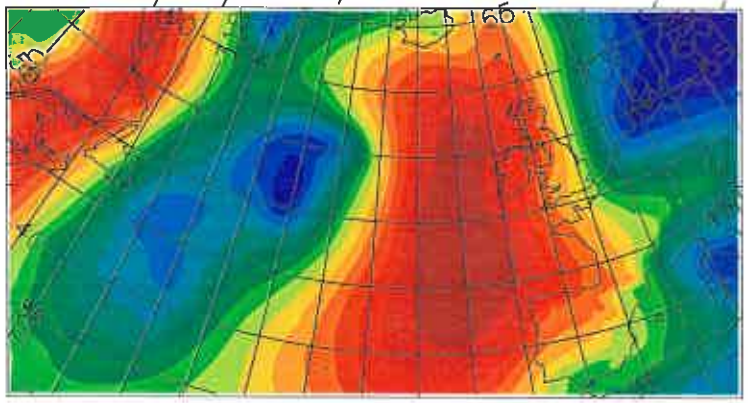

99400 100000 100600 101200 101800 102400 103000

XAATH Mean sea Level Atmos pressure at mean sea level
At 18Z on 13/10/1997, from 06Z on 13/10/1997

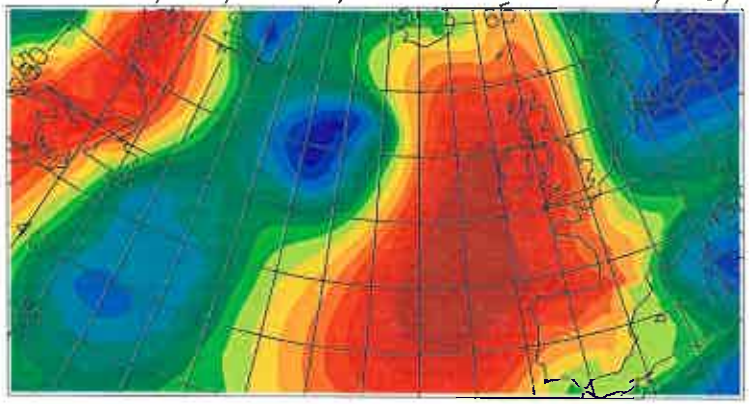

99400 100000 100600 101200 101800 102400 103000

XAATH Mean sea Level Atmos pressure at mean sea
At 00Z on 14/10/1997, from 06Z on 13/10/19

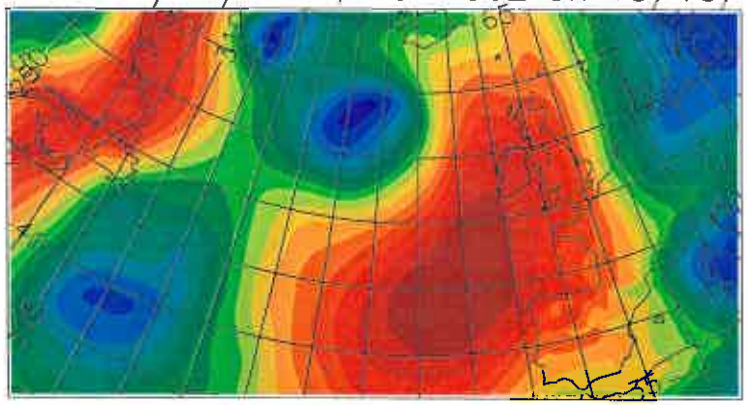

99400 100000 100600 101200 101800 102400 103000

XAATH Mean sea Level Atmos pressure at mean sea level
At 06Z on 14/10/1997, from 06Z on 13/10/1997

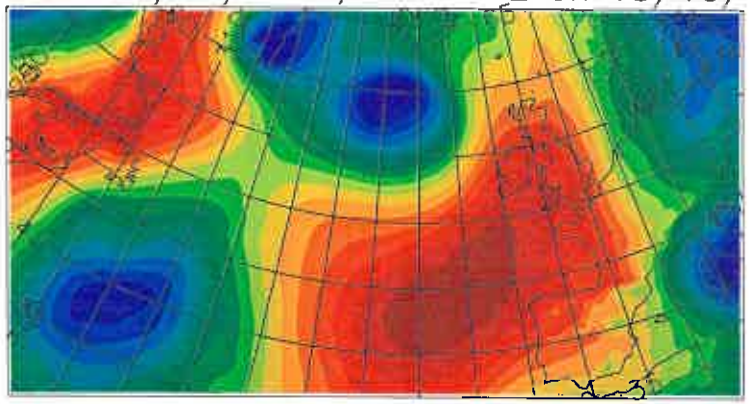

99400 100000 100600 101200 101800 102400 103000

XAATG Mean sea Level Atmos pressure at mean sea
At 06Z on 14/10/1997, from 06Z on 14/10/19

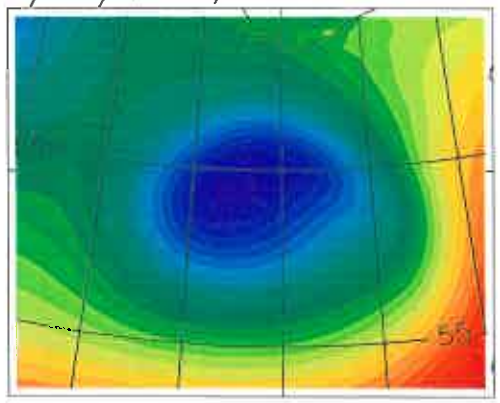

993997000100500900300700210500

XAATH Mean sea Level Atmos pressure at mean sea level
At 06Z on 14/10/1997, from 06Z on 13/10/1997

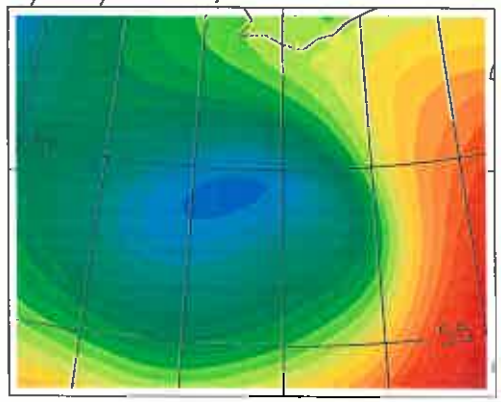

993997000100500900300700210500

XAATH Mean sea Level Atmos pressure at mean sea level
At 06Z on 14/10/1997, from 06Z on 13/10/1997

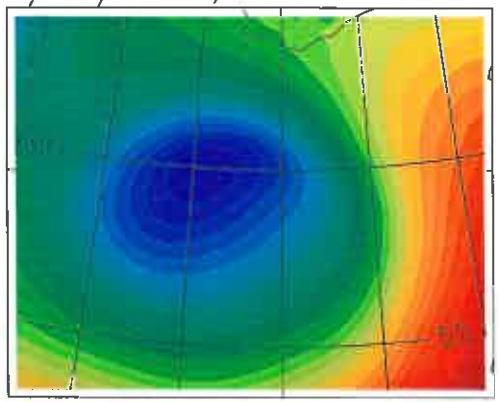

993997000100500900300700210500

CASE 13. 6Z 27/10/97 TO 6Z 28/10/97

Original Forecast

A cyclone with central surface pressure about 988hPa is located SE of Newfoundland at 6z 27/10/97. Over the subsequent 24 hours the analyses show that it moves very slowly eastwards while slowly filling; at 6z 28/10/97 its central pressure has reached about 994hPa. In the forecast the cyclone deepens significantly over the first 12 hours before starting to fill, so that by T+24 its central pressure is around 988hPa again. There is no significant position error however.

The trough corresponding to this system at 500hPa is slightly more extensive in the forecast than in the analyses. The same is true at 300hPa.

WV Image and PV Fields

The WV image on 250hPa shows a strong hook-shaped dry intrusion feature associated with this cyclone. This dry intrusion curves around the southern end of an oblong PV anomaly. At 400 & 500hPa the disposition of the PV maximum within this anomaly has shifted so that it lies within the dry intrusion. This is possibly in accordance with the view that the PV maximum at 250hpa represents a tropopause depression around which the dry intrusion circulates, while at 400hPa and lower levels, the PV signature of the dry intrusion itself is the dominant feature.

PV Adjustments & Results

In the forecast the cyclone does not start to fill until 12 hours after filling has started in the analyses. A rerun was performed in which the PV anomaly referred to above was scaled down by a factor of 0.6 on levels 250-500hPa. This approximately corrected the central surface pressure at T+24 and improved the central pressure value at all intermediate times.

The impact at 500hPa was negative. The forecast geopotential height for the cyclone centre at 500hPa was a little too high; in the rerun the central geopotential was increased rather than reduced. The impact on temperature at 500hPa was also slightly negative. The impact on geopotential and temperature at 300hPa was slightly positve in some localities and slightly negative in others.

The results of this case study have revealed the possiblity that upper-tropospheric PV adjustment can simultaneously have a positive impact on the surface forecast while having a negative impact aloft. This may suggest that to carry out upper-tropospheric PV adjustment alone without also adjusting PV at lower levels could be invalid in general.

CASE 14. 6Z 23/12/97 TO 6Z 25/12/97 Christmas Eve 97 Storm

Original Forecast

At 6z 23/12/97 the N Atlantic was dominated by a large low pressure system, with at least two low centres, which remained in roughly the same position over the subsequent 48 hours. A 'satellite' low extending from this system was located in mid-Atlantic at the latitude of S Spain. In the analyses this system developed two low centres which remained well separated and distinct as they moved towards the British Isles and then on towards Scandinavia.

The first of these lows deepened very rapidly from a central pressure of about 1000hPa at 18z 23/12/97 to about 974hPa at 18z 24/12/97. At 18z 24/12/97 it was centred over the N British Isles. This was the CE storm. 12 hours later (6z 25/12/97) it had reached Scandinavia and was still a distinct system. The second low also deepened rapidly and reached the W coast of Ireland at 6z 25/12/97.

The forecast development of these lows from 6z 23/12/97 went seriously astray. The positions of both low centres were much too far west up to T+24, and the first low centre deepened far too rapidly. Thereafter they both merged into the main N Atlantic low pressure complex and lost their identities as separate systems.

WV Image and PV Fields

The PV field at 300hPa (and 315K) at 6z 23/12/97 had a large complex area of high PV over the N Atlantic. Within this are two main PV anomalies, one of which ran across Newfoundland towards the SE, with its southern tip at about 38 deg latitude. This anomaly had considerable depth. It was a dominant feature on all levels down to 600hPa, and still visible at 700hPa and lower.

On the WV image this PV anomaly at has an associated dry intrusion curving around the southern end of it, the inner curve of the dry intrusion being apparently well matched with the curving edge of the PV anomaly at 300hPa & 315K. This dry intrusion was directly associated with the CE storm cyclone. The sequence of WV images shows that it rapidly elongated towards the British Isles and developed pronounced cyclonic curvature.

PV Adjustments & Results

Five reruns were carried out. None gave a positive impact on the forecast. In reruns 1,2 and 3 adjustments were made to the position or intensity of all or part of the large PV anomaly referred to above. The intensity adjustment had some impact on the intensity of the forecast cyclone, but none of these reruns had any significant effect on its trajectory. Rerun 4 used the Schmetz clear-sky pseudo WV image; this was converted to PV units by simple scaling, and a linear combination of this field and the original PV field was taken. This resulted in a much worse forecast development, with greatly increased position errors. In rerun 5 the position of another PV anomaly was adjusted; this had a negligible impact on the forecast. In the light of subsequent experience it is now considered that all of these PV adjustments were invalid. Further work on this case is envisaged.

6. CONCLUDING SUMMARY

The project to date has looked at 14 forecast cases. Six of these can be claimed to have yielded a positive impact on the surface pressure forecast, of which three appear to have been significant impacts, and the other three marginal. Of the three marginal cases, one actually gave a negative impact at 500hPa. All the positive impacts have been obtained as a result of scaling PV anomalies at upper tropospheric levels (generally 250-500hPa); no positive impacts have resulted from displacement of anomalies.

It appears that the PV/WV relation is not well understood, although some qualitative insight has been attained. There are certain types of dry feature which are frequently seen in WV images, and certain types of anomaly which are frequently seen in PV fields around the 250/300hPa level (or on the 330K isentropic surface), and the relationships of these characteristic dry features to the corresponding PV structures are also recognisable. The relation between PV anomalies and dry features is certainly not based on simple "superposition". Dry intrusion features usually fit around the flanks of PV anomalies at the 250/300hPa level; at lower levels (typically 400/450hPa) this phase relation tends to shift, and they may in fact appear to be superposed at these levels.

The concept of a "mismatch" between the PV and the WV image does not appear to be well-defined. In fact, no definite examples of "mismatch" can be seen among the 14 cases considered thus far, at least as far as positioning is concerned. In the light of the (admittedly vague) understanding of the PV -WV relation which has been arrived at, it appears that in every case the "fit" between the PV fields and the WV image looks reasonable, especially when the vertical structure of the PV distribution is taken into account. This is so, irrespective of how accurate the forecast was. This seems to suggest that the PV - WV image comparison may not provide any definite guidance as to how (or whether) PV anomalies should be adjusted at upper tropospheric levels.

However, it may well be that the PV - WV relation is often confused by the presence of cloud overlying dry intrusions as they descend into the troposphere, or by dry air becoming mixed with moist air. If such situations could readily be recognised then this may help to dispel the confusion surrounding this issue.

The PV inversion procedure also has numerous shortcomings, which are listed in chapter 4. One of the most significant is the pressure-surface formulation of the PV inversion scheme, which results in loss of consistency between the PV inversion domain's bottom boundary and the earth's surface.

Possibilities for further work

It seems worthwhile to carry out further case studies involving upper-tropospheric PV adjustment, or to re-examine some of the earlier cases in the light of what has been learned so far. Any further case studies would probably be carried out with the high-resolution global configuration of the UM. The following aspects should also be included in further case study investigations::

- Investigate PV adjustment at lower tropospheric levels, possibly guided by conceptual model analysis. In particular, attempt to apply lower tropospheric PV adjustment in the CE 97 case.

• Investigate the correlation between PV and potential temperature at the 850hPa level. It is alleged (private communication from T. Davies of UKMO; also Hoskins et al., 1985) that 850hPa potential temperature is related to WV imagery in the same sort of manner as upper tropospheric PV.

• Investigate the static stability and vorticity components of PV as separate fields, and the manner in which they are related to WV imagery.

• Consider possible additional data sources for lower tropospheric adjustment. Scatterometer winds have been mentioned in this connection - perhaps they could provide near-surface level wind adjustments which could be used in conjunction with upper-level wind adjustments from PV inversion.

• Attempt to utilise displacements derived from comparison of satellite and pseudo WV imagery.

Adjustment of Background Fields vs. Analyses

It has been commented that the attempt to improve forecasts by adjusting *analyses* is unlikely to be successful in general, because the analysis is substantially correct in most cases. This may, to some extent, explain why the results so far have shown little positive impact. The likelihood of obtaining positive impacts on forecasts may be enhanced by making adjustments to background fields rather than to analyses. Henceforth case studies will be carried out on this basis. The original forecast will be started from the background fields rather than from the analysis, and the rerun forecast from the adjusted background fields. Such an approach should also avoid any complications or uncertainties associated with the data assimilation process.

When and How should PV/WV methodology be applied?

The case study methodology employed so far in this project has included a priori knowledge of forecast errors in each case. The forecast is compared with the corresponding analyses, and this comparison provides part of the guidance by which the PV adjustments are arrived at. In order to test the methodology adequately, case studies should be carried out without the benefit of such hindsight. A set of rules is therefore required to enable decisions to be made as to (a) whether PV adjustment should be applied in any given case, and (b) if it is to be applied, how the PV should be adjusted. These rules should be based solely on information available at or before the analysis time. Ultimately, the only satisfactory solution to both of these problems would be to establish a quantitative relation between upper tropospheric PV fields and WV images. If the "correct" PV field could be deduced from the WV image, then by comparing this to the model's PV field the answers to both (a) and (b) would be obtained.

As yet, such a quantitative relation has not been well established (although progress towards this is being made, see section 3.3). An attempt to formulate qualitative guidelines was made by M. Demirtas, as discussed in section 3.1, although these guidelines are not precise enough to be of significant practical use. It is not yet possible to formulate any thing like an adequate set of qualitative guidelines on the basis of the work carried out so far in this project. However, the following points can

be made, all of which have been stated or implied in earlier sections of this report, but we will draw them together here.

- PV/WV methodology is useful only in connection with cyclonic systems.

- It can be used at any stage of cyclonic development, but is particularly pertinent for the early stages.

- It is most successfully applied to isolated cyclonic systems, associated with isolated pv anomalies.

- Scaling up a PV anomaly will deepen a cyclone over its subsequent evolution (typically 36-48 hours duration); scaling down the anomaly will make the cyclone shallower. Generally, a PV change of around 2 PVU at the location of the anomaly maximum produces a change of around 5mb in the central pressure, this change being maintained over the subsequent development.

- The effect of displacing of a PV anomaly will be to alter the track of the cyclone in an apparently unpredicatble manner. So far, all attempts at displacement of anomalies have had negative impacts on the forecast.

- On the basis of the cases studied so far in this project, it appears that intensity errors are generally much more significant than position errors, over 24-48 hours forecast ranges.

- As yet it has not been possible to make a judgement at analysis time as to whether a cyclone will be incorrectly developed by the forecast; hence it has not yet been possible to decide in advance whether PV adjustment is appropriate in any given case. This issue is being addressed by A.T.Semple, via conceptual model analysis in conjunction with satellite imagery.

References

Appenzeller, C. and Davies, H.C. (1992), Structure of Stratospheric Intrusions into the Troposphere, *Nature,* **358,** 570-572

Demirtas, M. (1996), Sensitivity of Short-Range Forecasts to Local Potential Vorticity Modifications, *Ph.D. Thesis, University of Reading*

Demirtas, M. and Thorpe, A.J. (1997), Sensitivity of Short-Range Forecasts to Local Potential Vorticity Modifications,
JCMM Internal Report 71, University of Reading

Davis, C.A. and Emanuel, K.A. (1991), Potential Vorticity Diagnostics of Cyclogenesis, *Mon. Wea. Rev.,* **119,** 1929-1953

Fehlmann, R. and Davies, H.C. (1997), Misforecasts of Synoptic Systems: Diagnosis via PV Retrodiction, *Mon. Wea. Rev.*, **125,** 2247-2264

Fehlmann, R. (1997), Dynamics of Seminal PV Elements, *Doctoral Thesis,*
ETH Zurich

Georgiev, C.G. (1996), Correlation of Meteosat WV Data to Middle Troposphere PV Anomalies, *Proc. EUMETSAT Met. Satellite Data Users Conf., Vienna,*
EUM P19, 129-136

Griffiths, M., Thorpe, A., and Browning, K. (1998), Convective Destabilisation by a Tropopause Fold Diagnosed using PV Inversion,
JCMM Internal Report 96, University of Reading

Hoffman, R.N., Liu, Z., Louis, J-F., and Grassotti, C. (1995), Distortion Representation of Forecast Errors, *Mon. Wea. Rev.,* **123,** 2758-2770

Hoskins, B.J., McIntyre, M.E., Robertson, A.W. (1985), On the Use and Significance of Isentropic Potential Vorticity Maps, *Q.J.R. Met. Soc.,* **111**, 877-946

Li, Y. et al. (1998), A Study on Assimilating Potential Vorticity Data,
Tellus, **50A,** 490-506

Morgan, M.C.,and Nielsen-Gammon J.W. (1998), Using Tropopause Maps to Diagnose Mid-Latitude Weather Systems,
Mon. Wea. Rev. **126,** 2555-2579

Pankiewicz, G.S. (1997), Satellite Imagery Pattern Recognition Products for NWP,
FR Tech. Report 206, UK Met Office

Rosting, B., Sunde, J., and Midtbo, H.K. (1996), Monitoring of NWP Models by use of Satellite Data, *Meteorol. Appl.,* **3,** 331-340

Semple, A.T. (1998), Conceptual Models of Cyclogenesis,
JCMM Internal Report 92, University of Reading

Schmetz, J. and van de Berg, L. (1994), Upper Tropospheric Humidity Observations from Meteosat compared with Short-Term Forecast Fields,
Geophys. Res. Lett., **21,** 573-576

Ziemanski, M. (1994), Potential Vorticity Inversion,
JCMM Internal Report 39, University of Reading

CURRENT JCMM INTERNAL REPORTS

This series of JCMM Internal Reports, initiated in 1993, contains unpublished reports and also versions of articles submitted for publication. The complete set of Internal Reports is available from the National Meteorological Library on loan, if required.

1. **Research strategy and programme**
   K A Browning et al
   January 1993

2. **The GEWEX Cloud System Study (GCSS)**
   GEWEX Cloud System Science Team
   January 1993

3. **Evolution of a mesoscale upper tropospheric vorticity maximum and comma cloud from a cloud-free two dimensional potential vorticity anomaly**
   K A Browning
   January 1993

4. **The global energy and water cycle**
   K A Browning
   July 1993

5. **Structure of a midlatitude cyclone before occlusion**
   K A Browning and N Roberts
   July 1993

6. **Developments in systems and tools for weather forecasting**
   K A Browning and G Szejwach
   July 1993

7. **Diagnostic study of a narrow cold frontal rainband and severe winds associated with a stratospheric intrusion**
   K A Browning and R Reynolds
   August 1993

8. **Survey of perceived priority issues in the parametrizations of cloud-related processes in GCMs**
   K A Browning
   September 1993

9. **The effect of rain on longwave radiation**
   I Dharssi
   September 1993

10. **Cloud microphysical processes - a description of the parametrization used in the large eddy model**
    H Swann
    October 1993

11. **An appreciation of the meteorological research of Ernst Kleinschmidt**
    A J Thorpe
    May 1992

12. **Potential vorticity of flow along the Alps**
    A J Thorpe, H Volkert and Dietrich Heimann
    August 1992

13. **The representation of fronts**
    A J Thorpe
    January 1993

14. **A parametrization scheme for symmetric instability: test for an idealised flow**
C S Chan and A J Thorpe
February 1993

15. **The Fronts 92 Experiment: a Quicklook Atlas**
Edited by T D Hewson
November 1993

16. **Frontal wave stability during moist deformation frontogenesis**
Part 1: Linear wave dynamics
C H Bishop and A J Thorpe
May 1993

17. **Frontal wave stability during moist deformation frontogenesis**
Part 2. The suppression of non-linear wave development
C H Bishop and A J Thorpe
May 1993

18. **Gravity waves in sheared ducts**
S Monserrat and A J Thorpe
October 1993

19. **Potential vorticity and the electrostatics analogy: quasi-geostrophic theory**
C Bishop and A J Thorpe
November 1993

20. **Recent advances in the measurement of precipitation by radar**
A J Illingworth
April 1993

21. **Micro-physique et givrage: cloud microphysics and aircraft icing**
A J Illingworth
May 1993

22. **Differential phase measurements of precipitation**
M Blackman and A J Illingworth
May 1993

23. **Estimation of effective radius of cloud particles from the radar reflectivity**
N I Fox and A J Illingworth
May 1993

24. **A simple method of Dopplerising a pulsed magnetron radar**
A Hua, A J Illingworth and J Eastment
November 1993

25. **Radiation and polar lows**
George C Craig
February 1994

26. **Collected preprints submitted to the International Symposium on the Life Cycles of Extratropical Cyclones; Bergen, Norway, 27 June - 1 July 1994**
April 1994

27. **Convective frontogenesis**
Douglas J Parker and Alan J Thorpe
April 1994

28. **Improved measurement of the ice water content in cirrus using a total water evaporator**
Philip R A Brown and Peter N Francis
April 1994

29. **Mesoscale effects of a dry intrusion within a vigorous cyclone**
K A Browning and B W Golding
April 1994

30. **GEWEX Cloud System Study, Science Plan**
May 1994

31. **Parametrization of momentum transport by convectively generated gravity waves**
R Kershaw
May 1994

32. **Mesoscale Modelling Newsletter No 5**
May 1994

33. **Observations of the mesoscale sub-structure in the cold air of a developing frontal cyclone**
K A Browning, S A Clough, C S A Davitt, N M Roberts and T D Hewson
May 1994

34. **Longwave radiative forcing of a simulated tropical squall line**
Imtiaz Dharssi
July 1994

35. **On the nature of the convective circulation at a kata-cold front**
K A Browning
September 1994

36. **Collective preprints of papers submitted to the COST-75 International Seminar on Advanced Weather Radar Systems, Brussels, 20-23 September 1994**
November 1994

37. **Use of satellite imagery to diagnose events leading to frontal thunderstorms: Parts I and II of a case study**
K A Browning and N M Roberts
November 1994

38. **The role of spaceborne millimetre-wave radar in the global monitoring of ice cloud**
P R A Brown, A J Illingworth, A J Heymsfield, G M McFarquhar, K A Browning and M Gosset
December 1994

39. **Potential vorticity inversion**
Michal Ziemianski
October 1994

40. **Theory of mature tropical cyclones; a comparison between Kleinschmidt (1951) and Emanuel (1986)**
Suzanne L Gray
December 1994

41. **Dispersion and removal of pollutants during the passage of an atmospheric frontal system**
N R Gimson
December 1994

42. **The role of snow sublimation in frontogenesis**
D J Parker and A J Thorpe
December 1994

43. **Potential vorticity and the electrostatics Analogy: Ertel-Rossby formulation**
A J Thorpe and C H Bishop
December 1994

44. **Mesoscale aspect of extratropical cyclones: an observational perspective**
K A Browning
January 1995

45. **A polar low outbreak: evolution and mesoscale structures**
T D Hewson, G C Craig and C Claud
February 1995

46. **Generation of near-surface gusts of deep convection**
K Nakamura and R Kershaw
April 1995

47. **Attribution concepts applied to the Omega Equation**
S A Clough, C S A Davitt and A J Thorpe
June 1995

48. **Parametrization of mixed-phase cloud and precipitation**
Susan P Ballard and M Gerard Hutchinson
June 1995

49. **Short-range forecasting of stratocumulus: initialization prediction**
Susan P Ballard, Simon D Jackson and B Macpherson
June 1995

50. **Contributions of the JCMM/Dept of Meteorology Radar Group to the 27th AMS Radar Meteorology Conference, Vail October 1995**
June 1995

51. **Cold pools in shear**
Douglas J Parker
September 1995

52. **High-resolution analysis of frontal fracture**
K A Browning, S P Ballard and C S A Davitt
September 1995

53. **The albedo of broken cloud fields: calculations using a modified two stream radiation code**
Imtiaz Dharssi and Roy Kershaw
October 1995

54. **Parametrization of momentum transport by convection. I: theory and cloud modelling results**
R Kershaw and D Gregory
November 1995

55. **Variation of frontal structure along a cold front**
K A Browning and N M Roberts
November 1995

56. **Secondary frontal waves**
Douglas Parker
December 1995

57. **Objective fronts**
T D Hewson
March 1996

58. **Mesoscale analysis of the activation of a cold front during cyclogenesis**
K A Browning, N M Roberts and A J Illingworth
June 1996

59. **Investigation of different representations of rain in a 1-d evaporation model**
H Swann
May 1996

60. **Parametrization of diabatic processes in the inversion of the omega-equation**
M Athanassiadou and A J Thorpe
June 1996

61. **The role of the environmental flow in the development of secondary frontal cyclones**
I A Renfrew, A J Thorpe and A Joly
June 1996

62. **Consequences of the geostrophic momentum approximation on barotropic instability**
S Malardel, A J Thorpe and A Joly
June 1996

63. **Contributions to the AMS/RMS Conference on Mesoscale Processes**
Reading, 9-13 September 1996

64. **Vorticity and potential vorticity in stratified flows interacting with an isolated obstacle**
Jorge A Gutiérrez and A J Thorpe
September 1996

65. **Triple point development: two case studies**
Douglas Parker
September 1996

66. **Radar observations of wind-shear splitting within evolving atmospheric Kelvin-Helmholtz billows**
D Chapman and K A Browning
April 1997

67. **Cold frontal structure derived from radar wind profilers**
K A Browning, D Jerrett, J Nash, T Oakley and N M Roberts
May 1997

68. **The dry intrusion and its effect on the frontal, cloud and precipitation structure of extratropical cyclones**
K A Browning - Text of invited special lecture at the Spring Conference of the Meteorological Society of Japan, University of Tsukuba, 22 May 1997

69. **Met. Office Unified Model data, diagnostics, graphics programs, and other observational data available from the JCMM through the aegis of the Universities Weather Research Network (UWERN).** (Plus supplement)
Peter Panagi and Ed Dicks
June 1997

70. **Contributions of the JCMM/Dept of Meteorology Radar Group to the 28th AMS Radar Meteorology Conference.** Austin, Texas
September 1997

71. **Sensitivity of short-range weather forecasts to local potential vorticity modifications**
Meral Demirtas and Alan Thorpe
July 1997

72. **Objective identification of frontal wave cyclones**
T D Hewson
August 1997

73. **Attribution and its application to mesoscale structure associated with tropopause folds**
A J Thorpe
September 1997

74. **The role of the environmental flow in the development of secondary frontal cyclones**
Ian A Renfrew, Alan J Thorpe and Craig H Bishop
September 1997

75. **Potential vorticity: a short history of its definitions and uses**
Alan J Thorpe and Hans Volkert
September 1997

76. **Superposing semi-geostrophic potential vorticity anomalies**
H R Birkett and A J Thorpe
September 1997

77. **Short period forecasting of catchment-scale precipitation.**
Part 1: the role of Numerical Weather Prediction
M A Pedder, M Haile and A J Thorpe
September 1997

78. **Verification of the tracking technique used in an experimental cloud motion wind inferring system**
Z Wang, K A Browning and G A Kelly
October 1997

79. **A preliminary study of Fourier series analysis for cloud tracking with GOES high temporal resolution images**
Z Wang
October 1997

80. **Analysis of an ex-tropical cyclone after reintensifying as a warm-core extratropical cyclone**
K A Browning, G Vaughan and P Panagi
November 1997

81. **A JCMM overview of FASTEX IOPs**
S A Clough, H W Lean, N M Roberts, H Birkett, J-P Chaboureau, R Dixon, M Griffiths, T D Hewson and A Montani
January 1998

82. **Programs for PV inversion and modification**
Meral Demirtas
December 1997

83. **Release of potential shearing instability in warm frontal zones**
D Chapman and K A Browning
February 1998

84. **The European Cloud-Resolving Modelling Programme (EUCREM)**
Summary Report from the coordinator
P W White
April 1998

85. **A frontal wave database**
T D Hewson
April 1998

86. **Layering observed in dropsoundings from IOP 1 of Fronts 92**
S A Clough
May 1998

87. **Use of wind-shear displays for Doppler radar data**
D Chapman and K A Browning
May 1998

88. **Radar estimates of rainfall rates at the ground in bright band and non-bright band events**
T J Smyth and A J Illingworth
June 1998

89. **Correction for attenuation of radar reflectivity using polarisation data**
T J Smyth and A J Illingworth
June 1998

90. **The effects of convection on chemical reactions and precipitation scavenging**
Neil R Gimson
July 1998

91. **How to use the display program DISP**
Nigel Roberts
August 1998

92. **Conceptual models of cyclogenesis**
Adrian T Semple
August 1998

93. **Observations of oblate hail using dual polarisation radar and implications for hail detection schemes**
T J Smyth, T M Blackman and A J Illingworth
September 1998

94. **The semigeostrophic diagnosis of vertical motion. Part I: Formulation and co-ordinate transformations**
Mike A Pedder and Alan J Thorpe
September 1998

95. **The semigeostrophic diagnosis of vertical motion. Part II: Results for an idealised baroclinic wave life cycle**
Alan J Thorpe and Mike A Pedder
September 1998

96. **Convective destabilisation by a tropopause fold diagnosed using potential vorticity inversion**
Morwenna Griffiths, Alan Thorpe and Keith Browning
October 1998

97. **Forecast skill of the ECMWF model using targeted observations during FASTEX**
A Montani, A J Thorpe, R Buizza and P Unden
October 1998

98. **Observations and model simulations of the FASTEX IOP 16 frontal wave - effects of sublimation**
Sid A Clough, Humphrey W Lean, Nigel M Roberts and Richard M Forbes
December 1998

99. **The application of conceptual models in NWP**
Adrian T Semple
January 1999

100. **Mesoscale analysis of arc rainbands in a dry slot**
K A Browning and N M Roberts
January 1999

101. **Interaction of mesoscale tropopause depressions with a warm-core cyclone: observational and model analyses, and sensitivity to analysis errors**
K A Browning, A J Thorpe, A Montani, D Parsons, M Griffiths, P Panagi and E M Dicks
February 1999

102. **Use of water vapour imagery and PV inversion to adjust initial conditions in NWP**
Sean J Swarbrick
February 1999

Met Office Joint Centre for Mesoscale Meteorology Department of Meteorology
University of Reading PO Box 243 Reading RG6 6BB United Kingdom
Tel: +44 (0)118 931 8425 Fax: +44 (0)118 931 8791
www.metoffice.com